A tunable human intestinal organoid system achieves controlled balance between self-renewal and differentiation

Li Yang[1,2,3,#], Xulei Wang[1,#], Xingyu Zhou[1], Hongyu Chen[1], Sentao Song[4], Liling Deng[1], Yao Yao[1], Xiaolei Yin*[1,2]

Supplementary Information

Contents include the following:

Supplementary Figures 1-20

Supplementary Tables 1-4

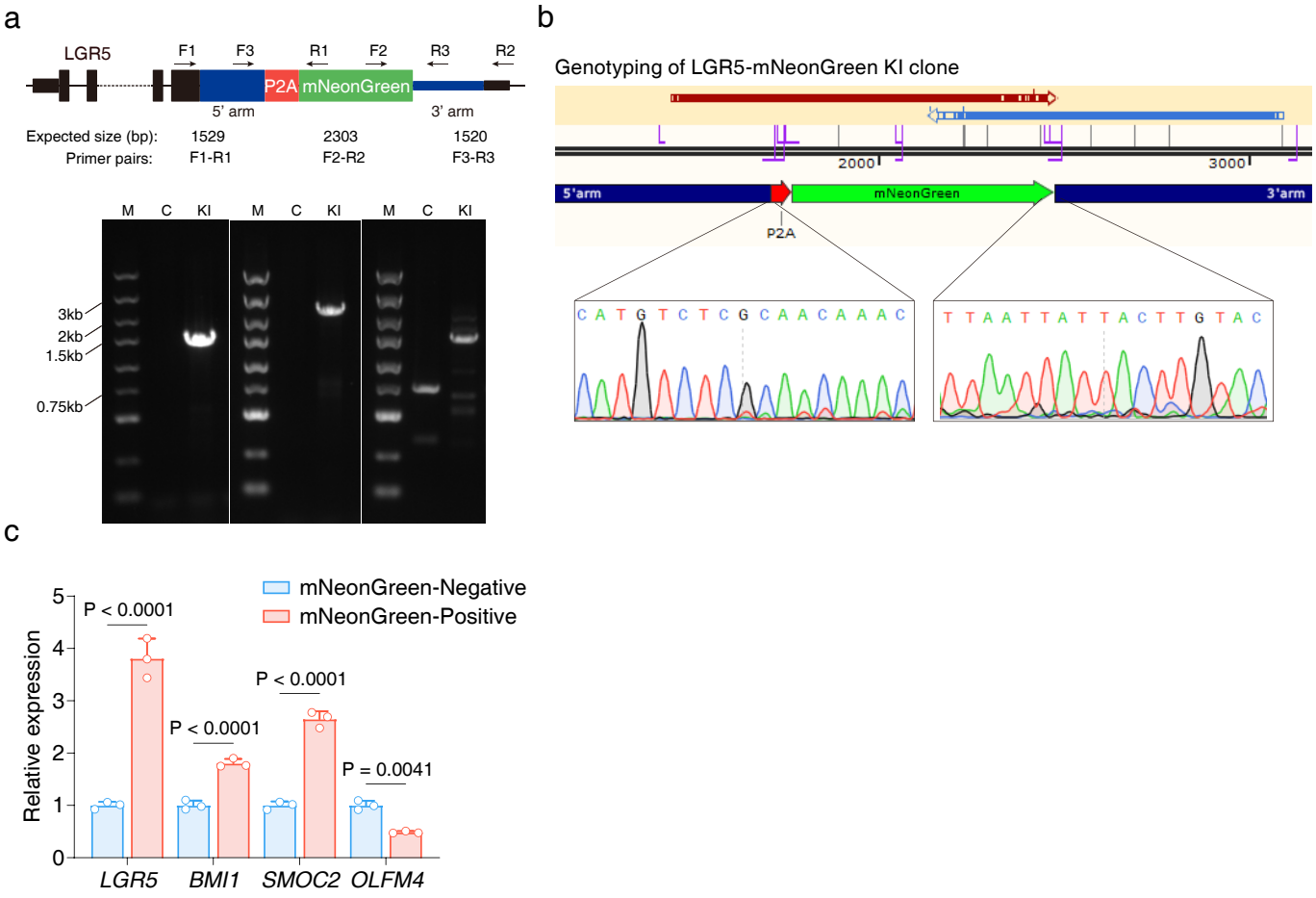

Supplementary Fig. 1 | Generation of LGR5-mNeonGreen organoids.

a Targeting strategy of the generation of LGR5-mNeonGreen reporter in TpC organoids. The upper panel shows the locations of PCR primers, and the lower panel shows gel electrophoresis of PCR products from Knock-in organoids using the indicated primers. Primers pairs F1/R1, F2/R2 and F3/R3 confirm the proper integration of mNeonGreen. Representative blots from three independent experiments. M, size marker; C, control organoid; KI, knock-in organoid. **b** Sequencing traces demonstrating the junction between the LGR5 gene and the knock-in sequence. **c** RT-qPCR quantification of stem cell marker expression levels. Two-way ANOVA analysis with Sidak's multiple comparisons test between mNeonGreen-negative cells and mNeonGreen-positive cells; data are presented as mean ± SD; data represents a representative experiment with *n* = 3 samples per condition. Source data for this Figure are provided as a Source Data file.

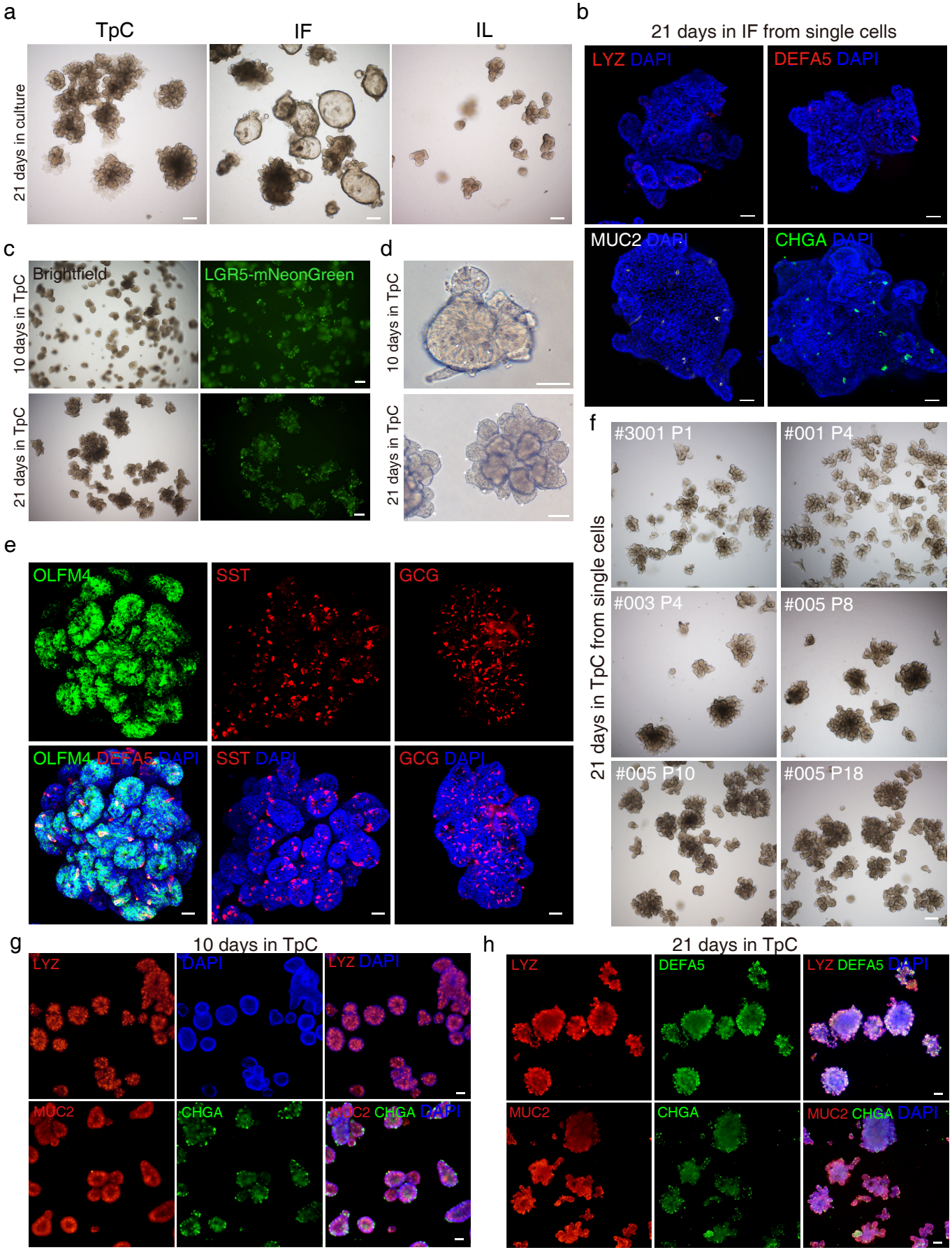
a
TpC
IF
IL
21 days in culture
b
21 days in IF from single cells
LYZ DAPI
DEFA5 DAPI
MUC2 DAPI
CHGA DAPI
c
10 days in TpC
21 days in TpC
Brightfield
LGR5-mNeonGreen
d
10 days in TpC
21 days in TpC
e
OLFM4
SST
GCG
OLFM4 DEFA5 DAPI
SST DAPI
GCG DAPI
f
21 days in TpC from single cells
#3001 P1
#001 P4
#003 P4
#005 P8
#005 P10
#005 P18
g
10 days in TpC
LYZ
DAPI
LYZ DAPI
MUC2
CHGA
MUC2 CHGA DAPI
h
21 days in TpC
LYZ
DEFA5
LYZ DEFA5 DAPI
MUC2
CHGA
MUC2 CHGA DAPI

Supplementary Fig. 2 | TpC organoid demonstrates enhanced stemness and increased cellular diversity.

a Representative brightfield images of organoids cultured in TpC, IF and IL patterning condition for 21 days from single cells. **b** Representative confocal images of Paneth cells (LYZ/DEFA5), goblet cell (MUC2) and EEC (CHGA) in IF condition for 21 days. **c** Representative brightfield and fluorescence images of organoids cultured in TpC condition for 10 and 21 days. **d** Representative images of Paneth-like cells with dark granules (arrows) at day 10 and extensive crypt-like budding structures (arrowheads) at day 21 in TpC organoids. **e** Representative confocal images of stem cell marker OLFM4, Paneth cell marker DEFA5 and enteroendocrine cell subtype markers SST and GCG in TpC organoids. **f** Representative brightfield images of intestinal organoids derived from multiple donors at different passages. **g-h** Uniformly expressed secretory lineage markers (LYZ, DEFA5, MUC2, and CHGA) in each 10 days (**g**) and 24 days (**h**) TpC organoid. All the representative images of this Figure were from at least three independent experiments. Scale bars, (**a, c, d** and **f-h**), 200 μM; (**b** and **e**), 50 μm.

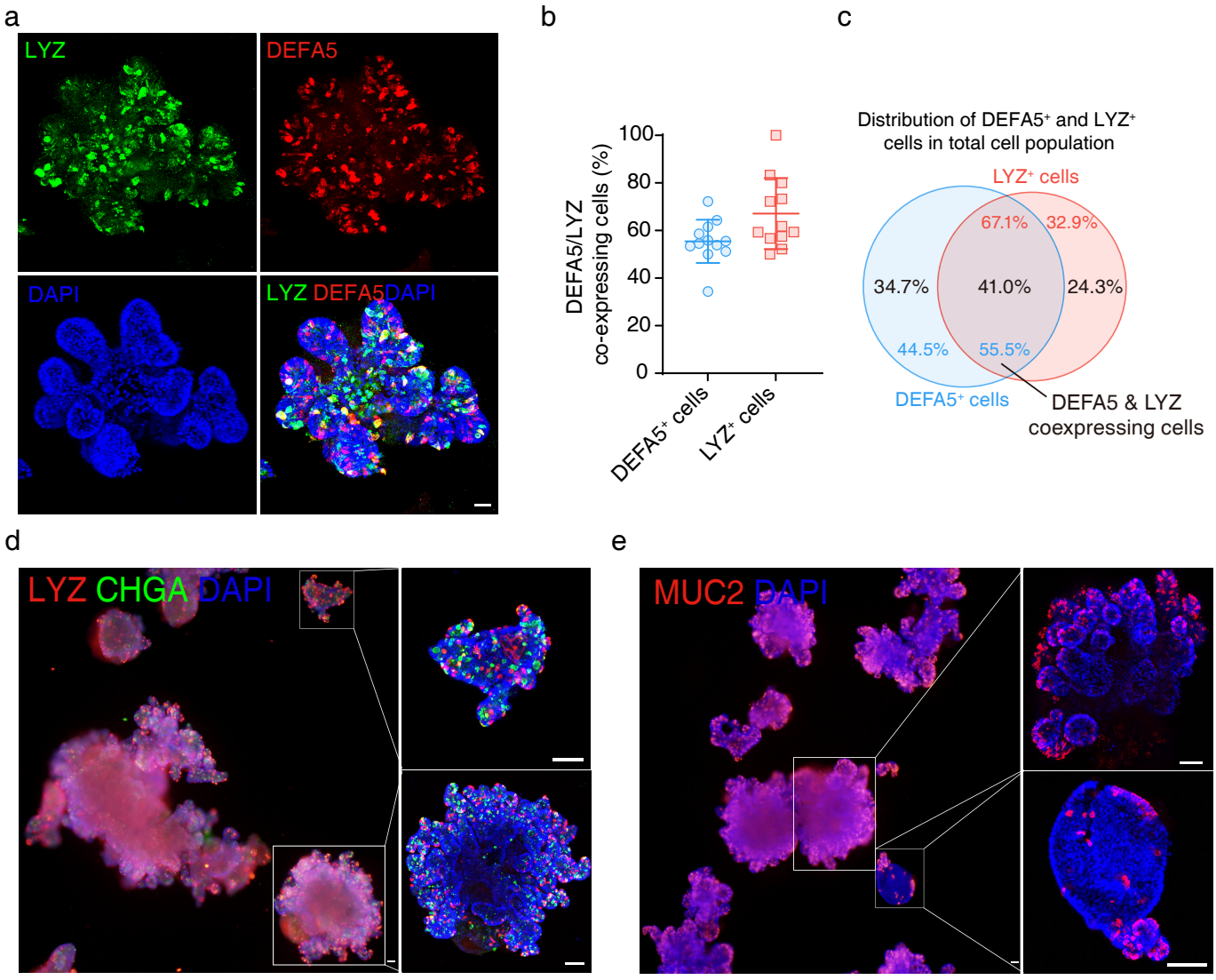

Supplementary Fig. 3 | Additional characterization of TpC organoids.

a Representative fluorescence images of Paneth cell markers (LYZ and DEFA5) in TpC organoids cultured for 21 days. Results reproducible for at least three biological replicates. **b** Quantification of the percentage of cells co-expressing DEFA5 and LYZ within DEFA5$^+$ and LYZ$^+$ cell populations. *n* = 12 samples. Data are presented as mean ± SD. Source data are provided as a Source Data file. **c** Venn diagram showing the distribution of DEFA5$^+$ and LYZ$^+$ cells in the total cell population that express either DEFA5 or LYZ, highlighting the proportion of cells co-expressing both markers (DEFA5$^+$ LYZ$^+$). **d-e** Immunofluorescence staining of Paneth cells (LYZ) and enteroendocrine cells (CHGA) (**d**), and goblet cells (MUC2) (**e**) in TpC organoids. Images include full views and amplified views of single organoids displaying round and budding structures. Representative images from three independent experiments. Scale bars, 50 μm.

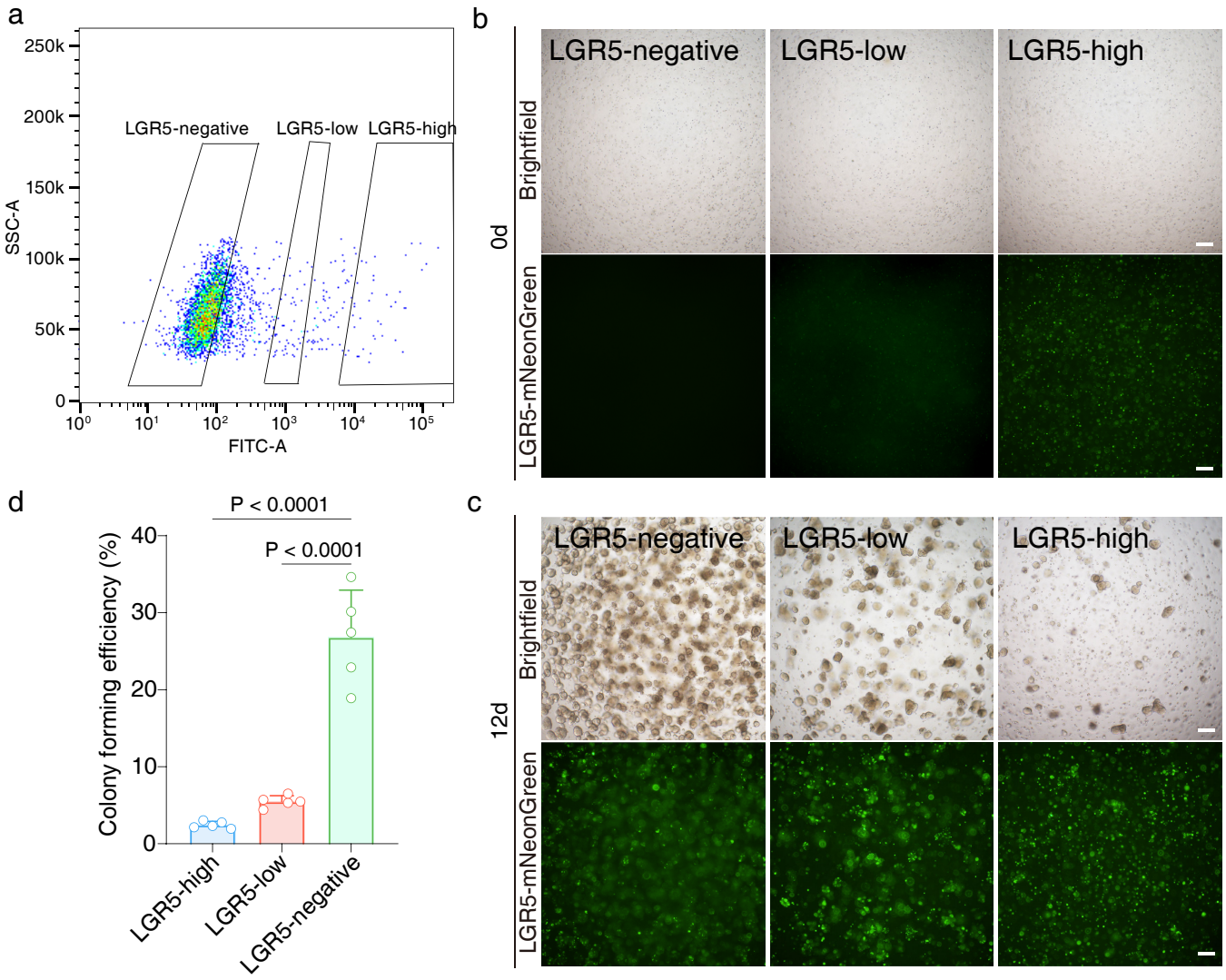

Supplementary Fig. 4 | TpC organoids originated from LGR5-positive and negative cells.

a FACS gating strategy for sorting LGR5-negative, LGR5-low, and LGR5-high cells in TpC organoids. **b** Brightfield and LGR5-mNeonGreen fluorescence images of cells sorted using the strategy indicated in (**a**), with 8000 cells seeded per well. **c** Brightfield and fluorescence images of organoids cultured in TpC condition for 12 days from single cells. Representative images of (**b** and **c**) from three independent experiments. Scale bar, 200 μm. **d** Quantification of the colony-forming efficiency of LGR5-negative, LGR5-low, and LGR5-high cells. One-way ANOVA with Dunnett's multiple comparisons test compared with LGR5-high cells; data are presented as mean ± SD; data represent a representative experiment with *n* = 5 samples per condition. Source data are provided as a Source Data file.

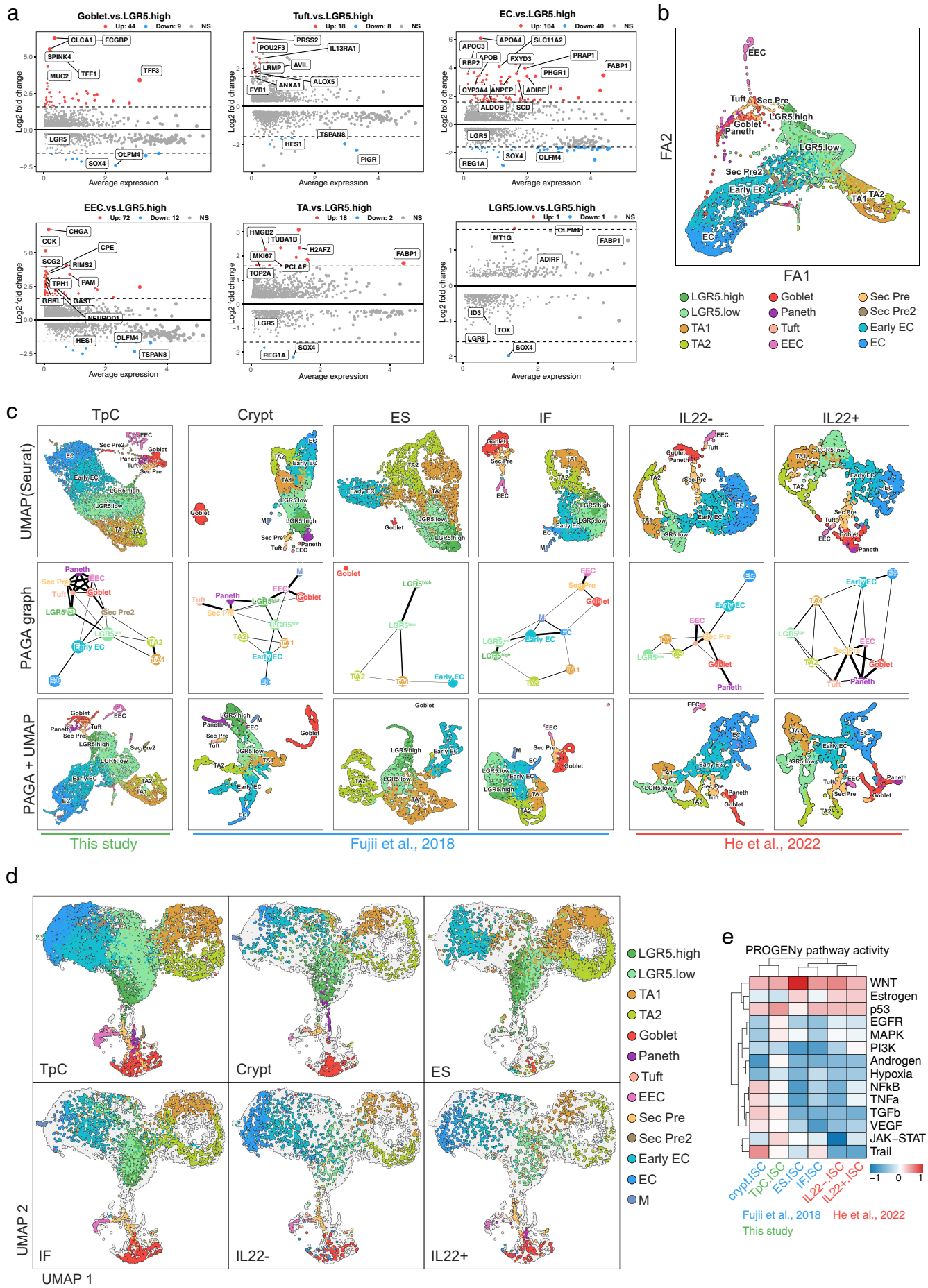
a
Goblet.vs.LGR5.high
Up: 44 Down: 9 NS
CLCA1 FCGBP SPINK4 MUC2 TFF1 TFF3 LGR5 OLFM4 SOX4
Tuff.vs.LGR5.high
Up: 18 Down: 8 NS
PRSS2 POU2F3 IL13RA1 LRMP AVIL ANXA1 ALOX5 FYB1 TSPAN8 HES1 PIGR
EC.vs.LGR5.high
Up: 104 Down: 40 NS
APOA4 SLC11A2 APOC3 APOB PRAP1 RBP2 FXYD3 FABP1 PHGR1 CYP3A4 ANPEP ADIRF ALDOB SCD LGR5 SOX4 OLFM4 REG1A
EEC.vs.LGR5.high
Up: 72 Down: 12 NS
CHGA CCK CPE SCG2 RIMS2 TPH1 PAM GRHL GAST NEUROD1 HES1 OLFM4 TSPAN8
TA.vs.LGR5.high
Up: 18 Down: 2 NS
HMGB2 TUBA1B H2AFZ MKI67 FABP1 PCLAF TOP2A LGR5 REG1A SOX4
LGR5.low.vs.LGR5.high
Up: 1 Down: 1 NS
OLFM4 MT1G FABP1 ADIRF ID3 TOX LGR5 SOX4
Log2 fold change
Average expression
b
FA1
FA2
EEC
Tuff
Sec Pre
Goblet
Paneth
LGR5.high
LGR5.low
Sec Pre2
Early EC
TA1
TA2
EC
LGR5.high
LGR5.low
TA1
TA2
Goblet
Paneth
Tuff
EEC
Sec Pre
Sec Pre2
Early EC
EC
c
TpC
Crypt
ES
IF
IL22-
IL22+
UMAP(Seurat)
PAGA graph
PAGA + UMAP
This study
Fujii et al., 2018
He et al., 2022
d
TpC
Crypt
ES
IF
IL22-
IL22+
UMAP 1
UMAP 2
LGR5.high
LGR5.low
TA1
TA2
Goblet
Paneth
Tuff
EEC
Sec Pre
Sec Pre2
Early EC
EC
M
e
PROGENy pathway activity
WNT
Estrogen
p53
EGFR
MAPK
PI3K
Androgen
Hypoxia
NFkB
TNFa
TGFb
VEGF
JAK–STAT
Trail
−1 0 1
crypt.ISC
TpC.ISC
ES.ISC
IF.ISC
IL22−.ISC
IL22+.ISC
Fujii et al., 2018
He et al., 2022
This study

Supplementary Fig. 5 | scRNA-seq analysis reveals cellular diversity and cell fate dynamics in human intestinal organoids.

a MA plots showing differentially expressed genes between different cell types and LGR5-high cells. **b** Force Atlas plot of TpC organoids from scRNA-seq analysis. **c** UMAP and PAGA trajectory analysis of the scRNA-seq data of ES, IF, IL, TpC organoids, and Crypt showing inferred developmental trajectories of cell types. Circle size indicates cell numbers, and line thickness indicates connectivity strength between clusters. **d** UMAP plot showing integrated analysis of scRNA-seq datasets of cells from ES, IF, IL, TpC organoids, and Crypt using the Seurat package. Clustering reveals distinct cell populations under different conditions. **e** Heatmap showing predicted PROGENy pathway activity of intestinal stem cells (ISCs) in ES, IF, IL, TpC organoids, and Crypt datasets.

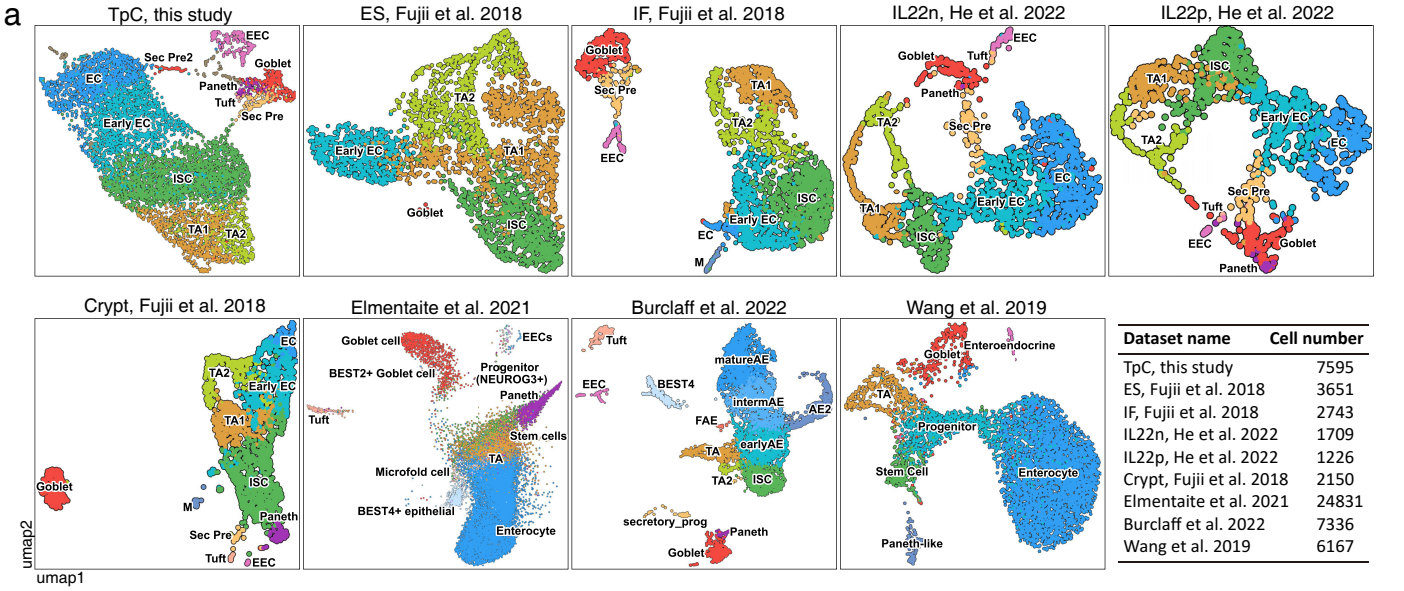

Dataset name	Cell number
TpC, this study	7595
ES, Fujii et al. 2018	3651
IF, Fujii et al. 2018	2743
IL22n, He et al. 2022	1709
IL22p, He et al. 2022	1226
Crypt, Fujii et al. 2018	2150
Elmentaite et al. 2021	24831
Burclaff et al. 2022	7336
Wang et al. 2019	6167

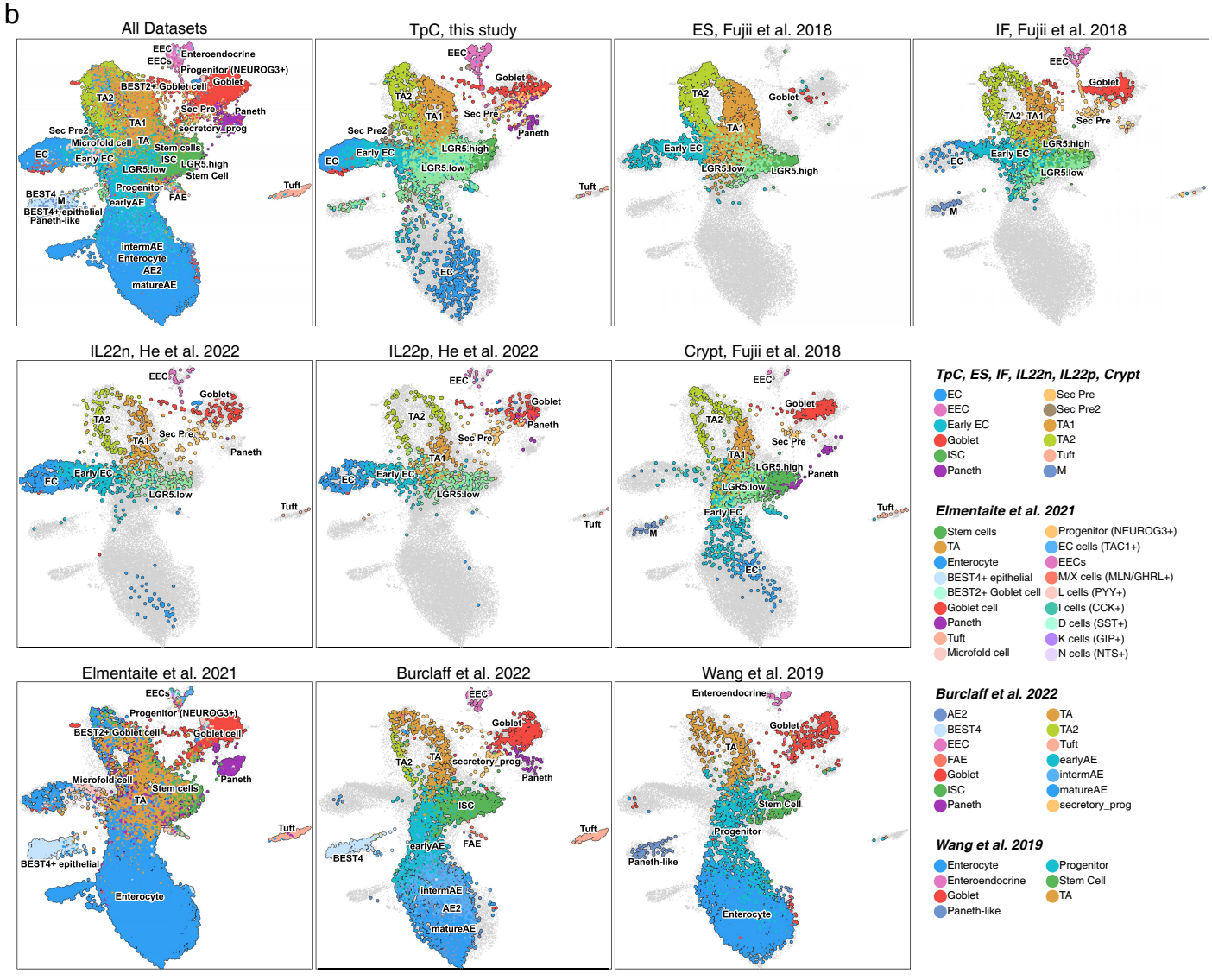

Supplementary Fig. 6 | Comparison of single-cell datasets from organoid and *in vivo* conditions.

a UMAP plot of single-cell RNA-seq datasets, including organoid datasets from TpC, ES, IF, IL22n, and IL22p conditions, as well as datasets from crypt and *in vivo* sources Each dataset is annotated according to originally provided annotation, the dataset names and the number of cells analyzed are provided in the accompanying table. **b** Harmony integration of single-cell RNA-seq datasets from organoid and *in vivo* conditions. The integrated UMAP plot shows the combined analysis of all datasets, with cells colored by their original dataset. Each dataset is individually represented to highlight the integration and clustering of similar cell types across different conditions. The legend indicates the color-coding for major cell types and datasets.

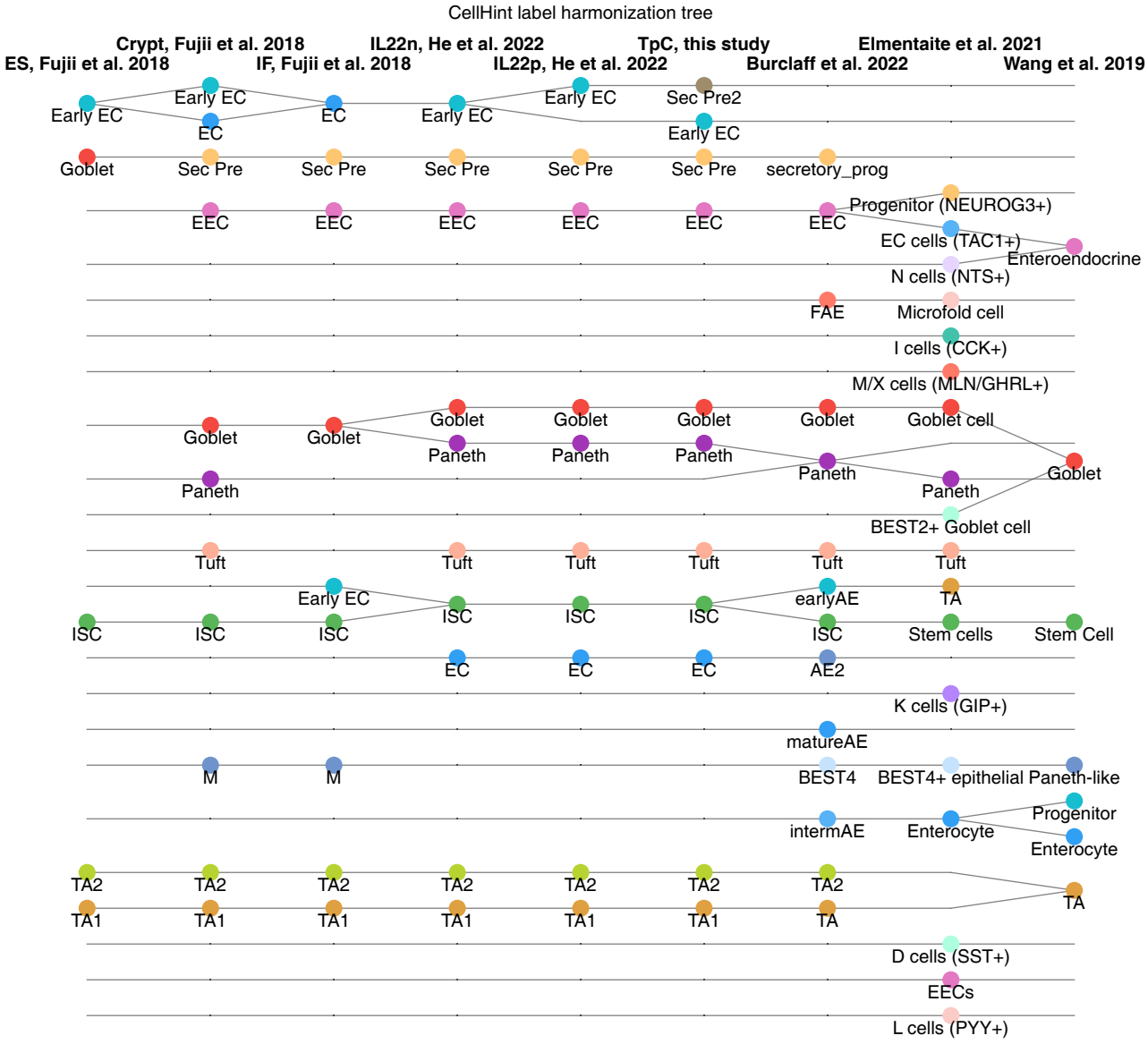

Supplementary Fig. 7 | CellHint-based harmonization of organoid and *in vivo* single-cell datasets.

Harmonization graph showing selected cell-type relationships across the organoid and *in vivo* datasets shown on top. Cell-type labels are colored according to their original annotation of cell types. The lines in the graph reflect the connections among transcriptionally similar cell types regardless of their names.

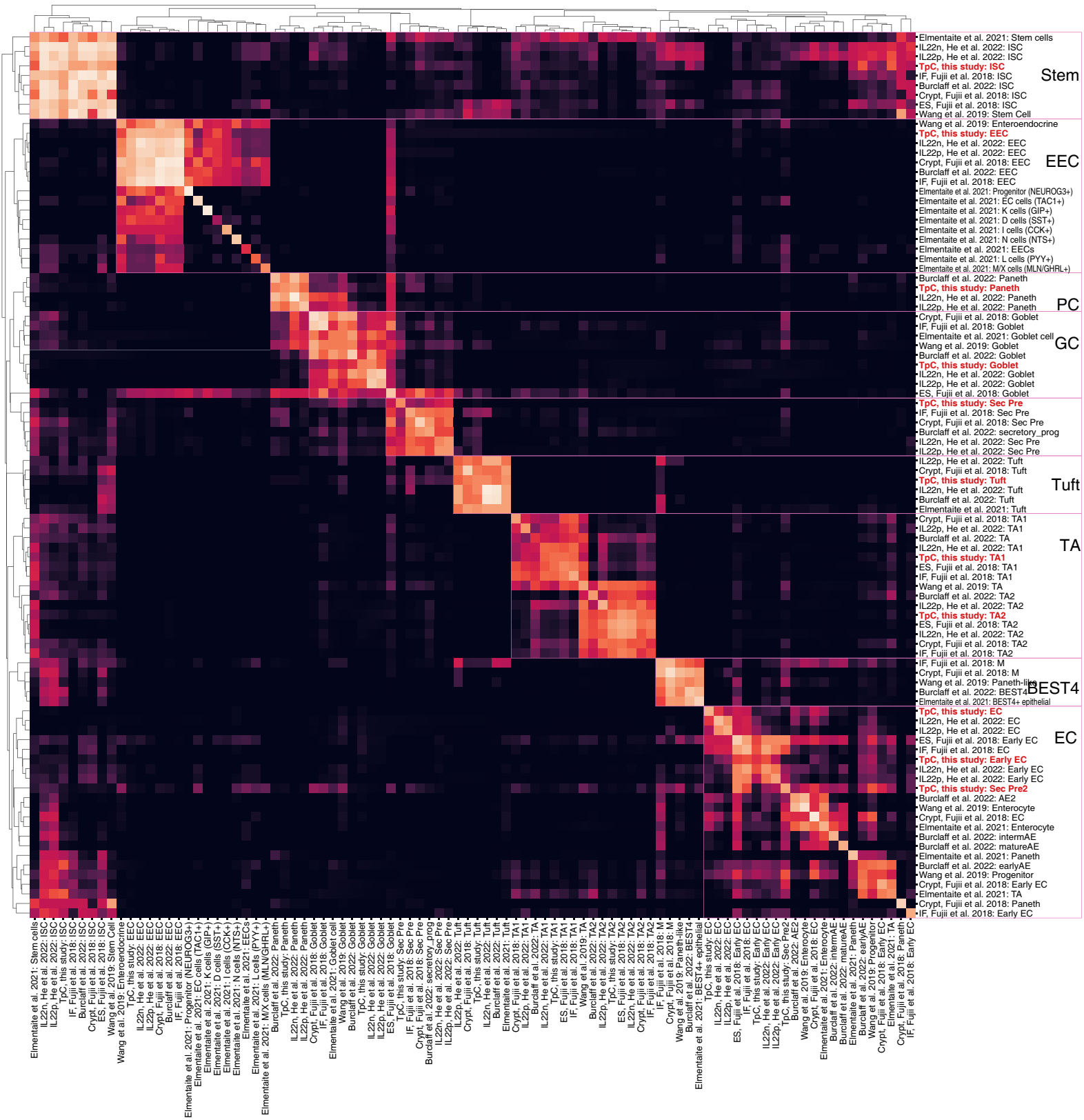

Supplementary Fig. 8 | Hierarchical clustering of cell types from organoid and *in vivo* datasets using CellHint.

Heatmap displaying the unsupervised hierarchical clustering of cell types based on their inferred similarities by CellHint. Each row or column represents a cell type. The color intensity indicates the degree of similarity between cell types across different datasets.

Supplementary Fig. 9 | Marker expression in organoid and *in vivo* single-cell clusters.

Dot plot showing the expression and percentage of cells expressing cell type-specific markers in clusters from organoid and *in vivo* datasets. Dot size represents the percentage of cells expressing each marker, while dot color indicates the normalized gene expression level.

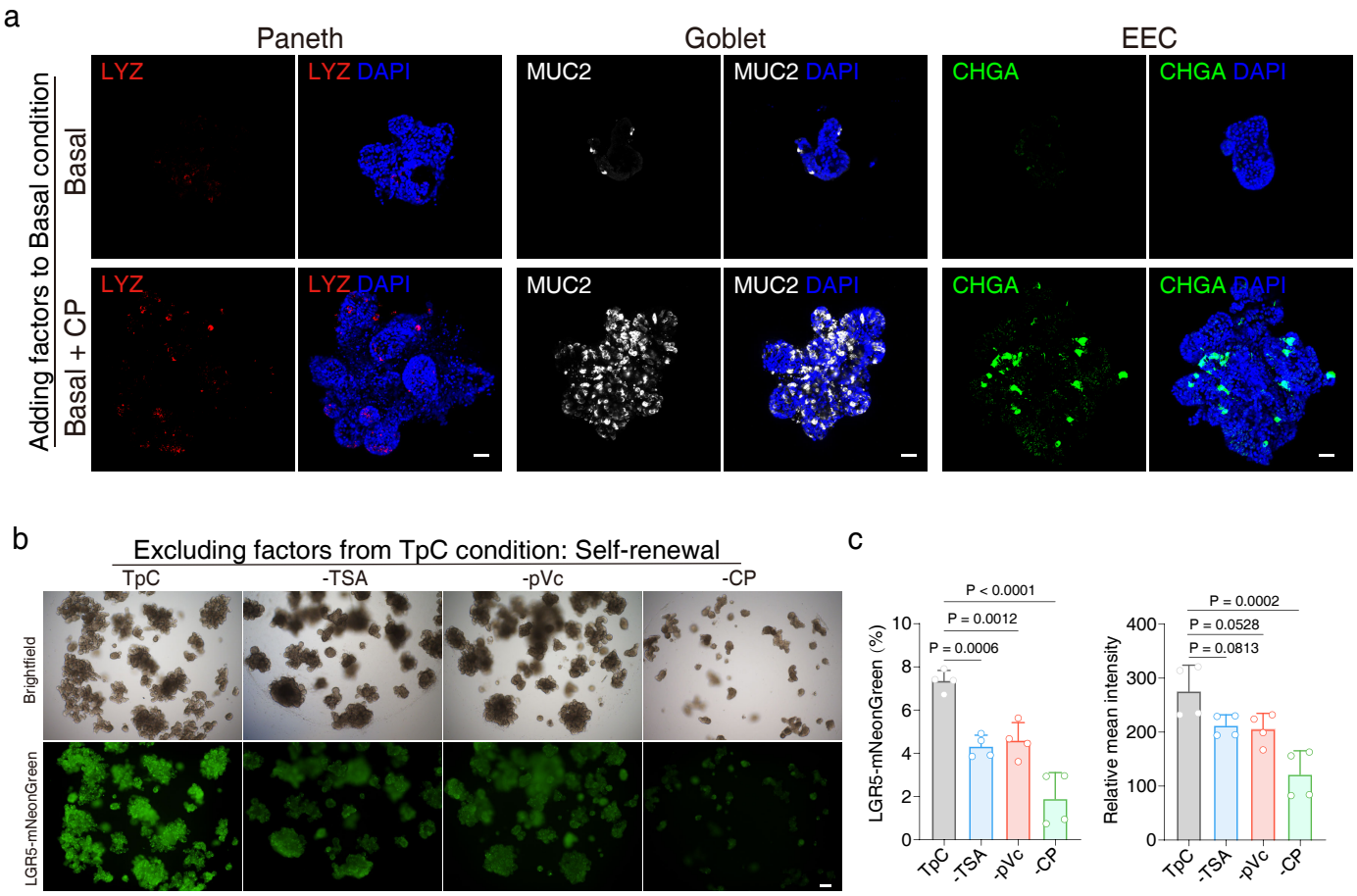

Supplementary Fig. 10 | TSA, pVc, and CP induce stemness maintenance in organoids.

a Representative images of Paneth cells (LYZ), goblet cells (MUC2), and enteroendocrine cells (CHGA) in organoids cultured under Basal conditions or with CP added. Representative images from three independent experiments. Scale bars, 50 μm. **b** Brightfield and mNeonGreen fluorescence images of organoids cultured for 28d in conditions as indicated. Representative images from four independent experiments. Scale bar, 200 μm. **c** Quantification of LGR5-mNeonGreen proportion and fluorescence intensity in organoids shown in (**b**). One-way ANOVA with Dunnett's multiple comparisons test compared with the TpC condition; data are presented as mean ± SD; representative experiment showing *n* = 4 samples from each condition. Source data are provided as a Source Data file.

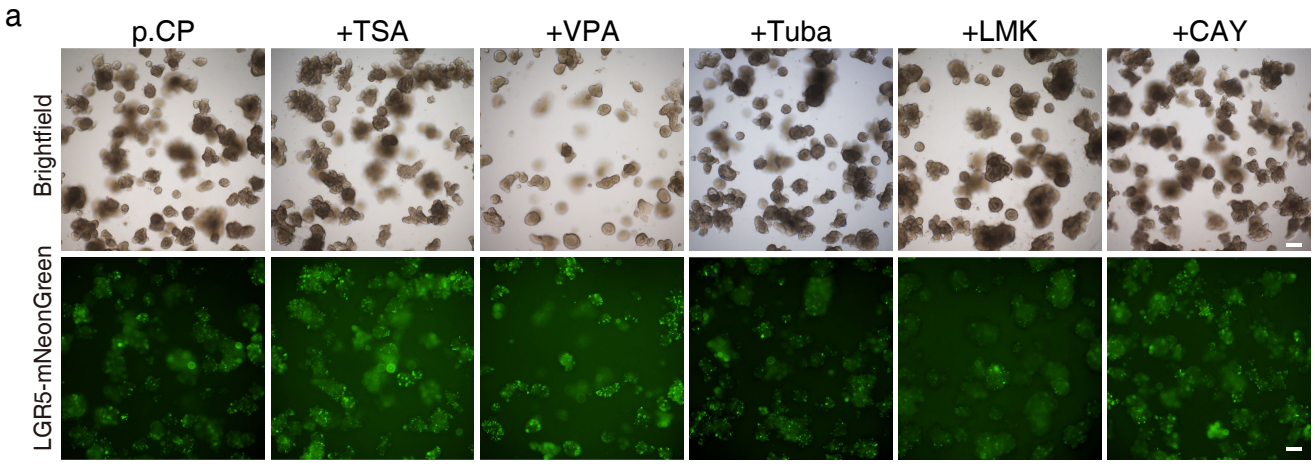

b

	Name	Target	Concentration
TSA	Trichostatin A	Pan HDAC	20 nM
VPA	Valproic Acid	Pan HDAC	0.5 mM
Tuba	Tubastatin A	HDAC6	1 μM
LMK	LMK235	HDAC4/5	100 nM
CAY	CAY10683	HDAC2	1 μM

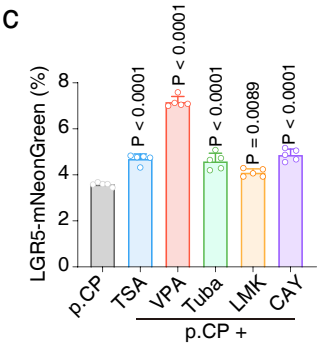

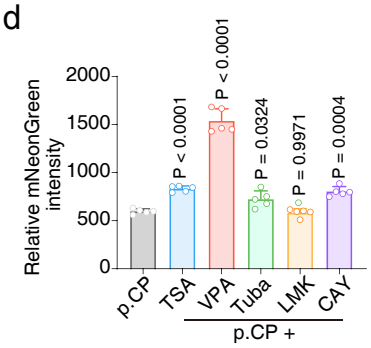

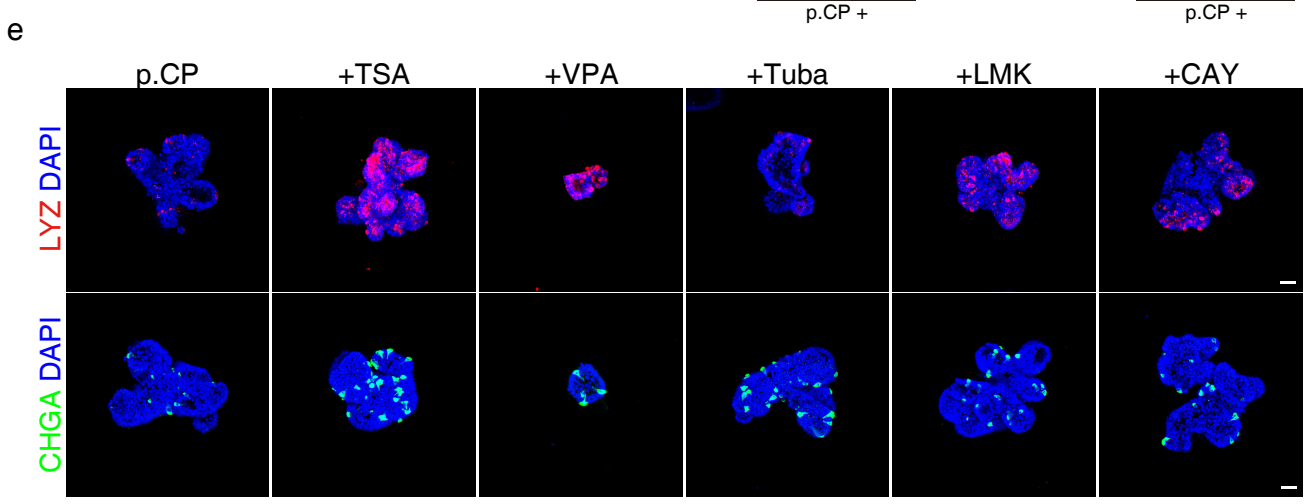

Supplementary Fig. 11 | Similar effects of HDAC inhibitors and TSA on organoids

a Morphology and fluorescence images of organoids cultured for 10 days from single cells showing the effects of TSA and other HDAC inhibitors. Representative images from five independent experiments. Scale bars, 200 μm. **b** HDAC inhibitors tested as in (**d**). **c-d** Quantification of LGR5-mNeonGreen percentage (**c**) and relative fluorescence intensity (**d**) in organoid of (**a**). One-way ANOVA with Dunnett's multiple comparisons test between each test condition with the condition without HDAC inhibitors (p.CP); data are presented as mean ± SD; representative experiment showing *n* = 5 samples from each condition. **e** Representative confocal images of Paneth cells and enteroendocrine cells in organoids cultured in conditions as indicated. Representative images from three independent experiments. Scale bars, 50 μm. Source data for this Figure are provided as a Source Data file.

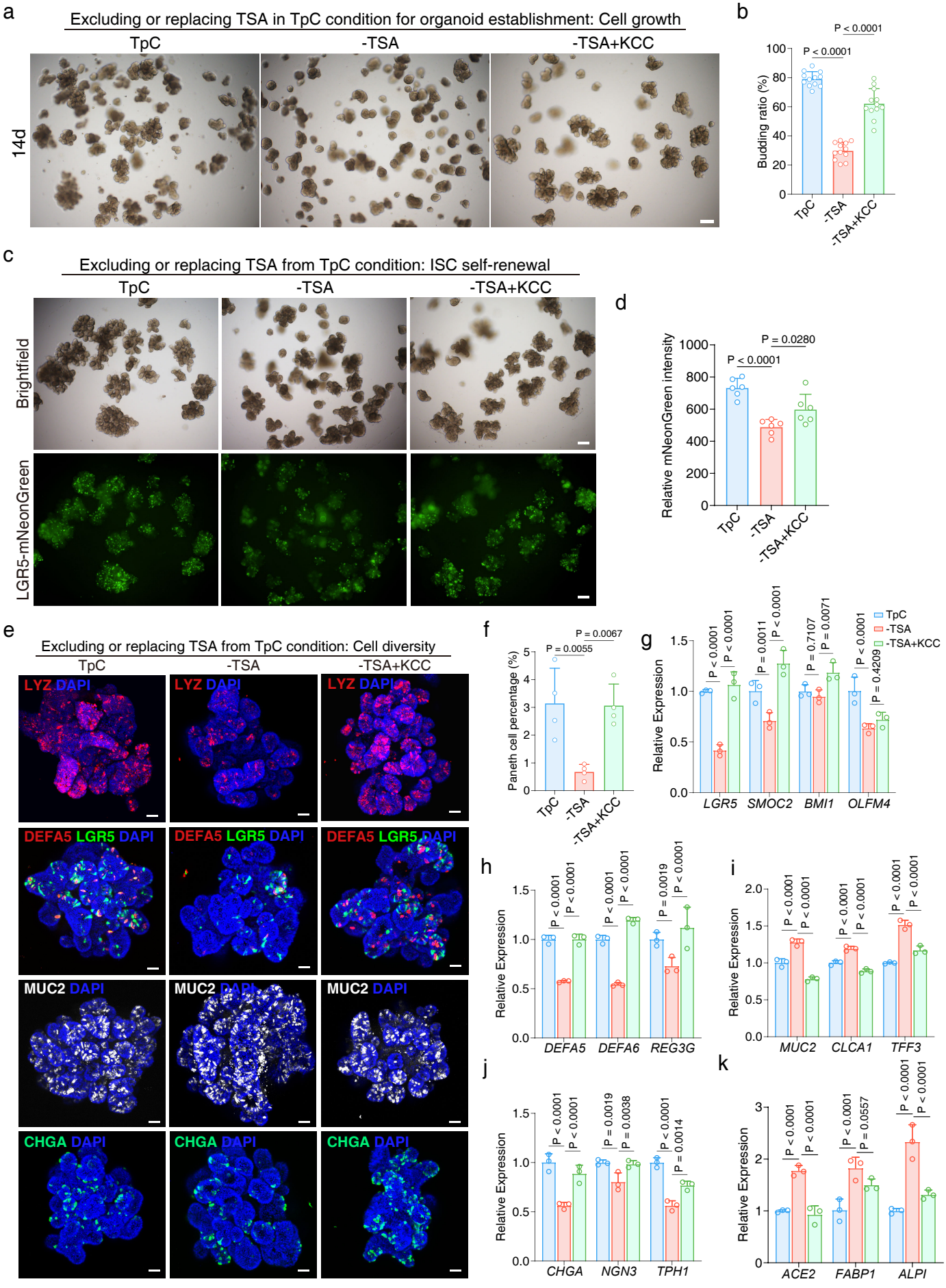
a
Excluding or replacing TSA in TpC condition for organoid establishment: Cell growth
TpC
-TSA
-TSA+KCC
14d
b
P < 0.0001
P < 0.0001
Budding ratio (%)
100
80
60
40
20
0
TpC
-TSA
-TSA+KCC
c
Excluding or replacing TSA from TpC condition: ISC self-renewal
TpC
-TSA
-TSA+KCC
Brightfield
LGR5-mNeonGreen
d
P = 0.0280
P < 0.0001
Relative mNeonGreen intensity
1000
800
600
400
200
0
TpC
-TSA
-TSA+KCC
e
Excluding or replacing TSA from TpC condition: Cell diversity
TpC
-TSA
-TSA+KCC
LYZ DAPI
DEFA5 LGR5 DAPI
MUC2 DAPI
CHGA DAPI
f
P = 0.0067
P = 0.0055
Paneth cell percentage (%)
5
4
3
2
1
0
TpC
-TSA
-TSA+KCC
g
TpC
-TSA
-TSA+KCC
Relative Expression
1.5
1.0
0.5
0.0
P < 0.0001
P < 0.0001
P = 0.0011
P < 0.0001
P = 0.7107
P = 0.0071
P < 0.0001
P = 0.4209
LGR5
SMOC2
BMI1
OLFM4
h
Relative Expression
1.5
1.0
0.5
0.0
P < 0.0001
P < 0.0001
P < 0.0001
P < 0.0001
P = 0.0019
P < 0.0001
DEFA5
DEFA6
REG3G
i
Relative Expression
2.0
1.5
1.0
0.5
0.0
P < 0.0001
P < 0.0001
P < 0.0001
P < 0.0001
P < 0.0001
P < 0.0001
MUC2
CLCA1
TFF3
j
Relative Expression
1.5
1.0
0.5
0.0
P < 0.0001
P < 0.0001
P = 0.0019
P = 0.0038
P < 0.0001
P = 0.0014
CHGA
NGN3
TPH1
k
Relative Expression
3
2
1
0
P < 0.0001
P < 0.0001
P < 0.0001
P = 0.0557
P < 0.0001
P < 0.0001
ACE2
FABP1
ALPI

Supplementary Fig. 12 | MBD2 inhibitor KCC-07 presents similar effects as TSA

a Morphology images of organoids cultured for 14 days from single cells in conditions as indicated. KCC-07 (KCC): 10 μm. Representative images from six independent experiments. Scale bars: 200 μm. **b** Quantification of budding ratio in organoid of (**a**). One-way ANOVA with Dunnett's multiple comparisons test between each test condition with TpC condition; data are presented as mean ± SD; representative experiment showing *n* = 12 samples from each condition. **c** Brightfield and fluorescence images of organoids cultured for 28 days in conditions as indicated. Representative images from six independent experiments. Scale bars: 200 μm. **d** Relative fluorescence intensity in organoid of (**c**) were detected by FACS. One-way ANOVA with Dunnett's multiple comparisons test between each test condition and the TpC condition; data are presented as mean ± SD; representative experiment showing *n* = 6 samples from each condition. **e** Representative confocal images of LGR5-mNeonGreen stem cells, Paneth cells (LYZ and DEFA5), goblet cells (MUC2) and enteroendocrine cells (CHGA) in organoids cultured in conditions as indicated. Representative images from three independent experiments. Scale bars: 50 μm. **f** Percentages of Paneth cell in organoids shown in (**e**). One-way ANOVA with Dunnett's multiple comparisons test between each test condition and the pC condition; data are presented as mean ± SD; representative experiment showing *n* = 4 samples from each condition. **g-k** RT-qPCR quantification of markers for stem cell (**g**), Paneth cell (**h**), goblet cell (**i**), EEC (**j**) and EC (**k**) in organoids cultured in TpC, pC (-TSA), or -TSA+KCC conditions. Two-way ANOVA with Dunnett's multiple comparisons test between each condition and the pC condition; data are presented as mean ± SD; representative experiment showing *n* = 3 samples. Source data for this Figure are provided as a Source Data file.

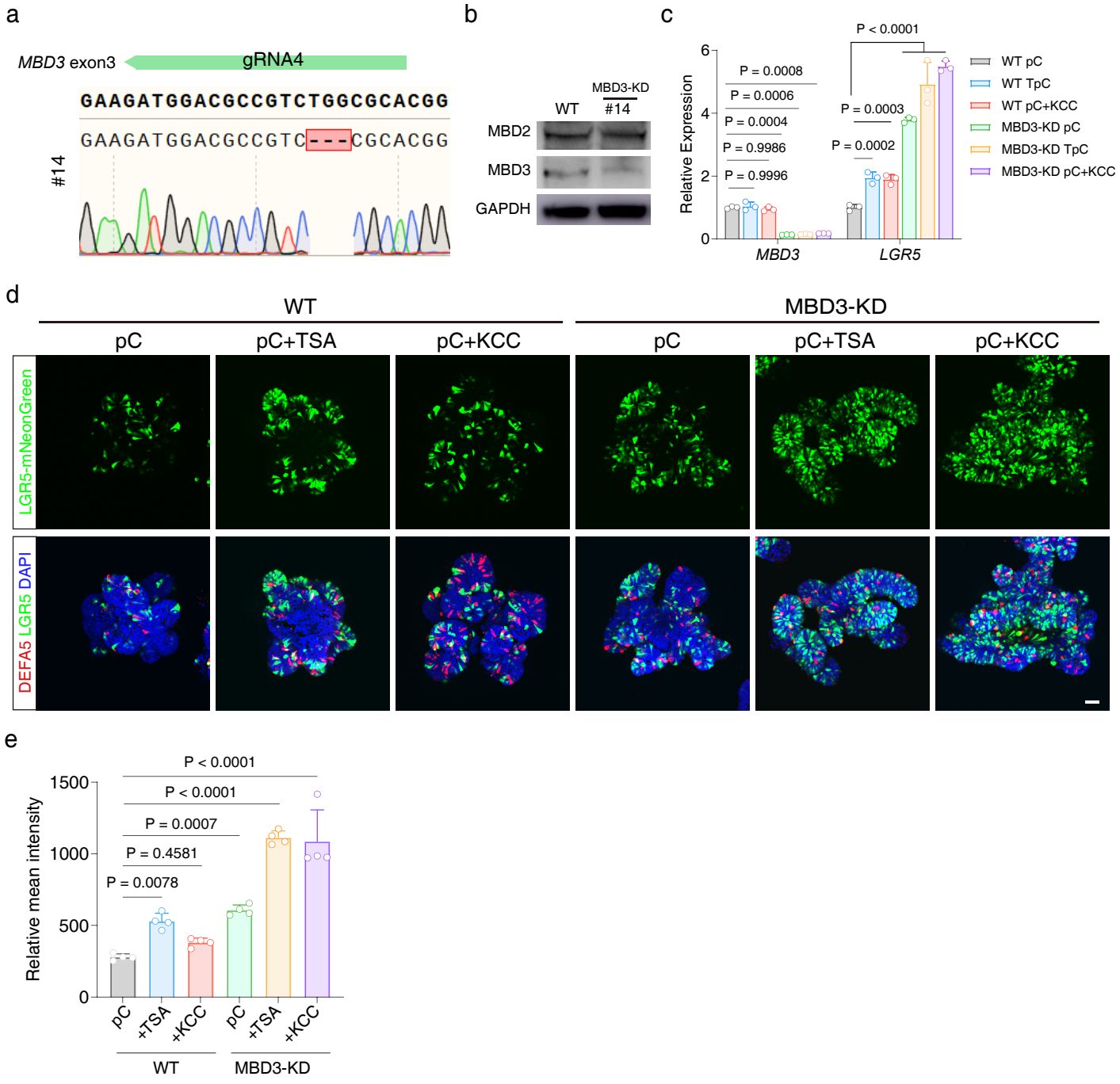
a
MBD3 exon3
gRNA4
GAAGATGGACGCCGTCTGGCGCACGG
GAAGATGGACGCCGTC---CGCACGG
#14
b
WT
MBD3-KD
#14
MBD2
MBD3
GAPDH
c
Relative Expression
P = 0.0008
P = 0.0006
P = 0.0004
P = 0.9986
P = 0.9996
P < 0.0001
P = 0.0003
P = 0.0002
MBD3
LGR5
WT pC
WT TpC
WT pC+KCC
MBD3-KD pC
MBD3-KD TpC
MBD3-KD pC+KCC
d
WT
MBD3-KD
pC
pC+TSA
pC+KCC
LGR5-mNeonGreen
DEFA5 LGR5 DAPI
e
Relative mean intensity
P < 0.0001
P < 0.0001
P = 0.0007
P = 0.4581
P = 0.0078
pC
+TSA
+KCC
WT
MBD3-KD

Supplementary Fig. 13 | Inhibition of MBD3 promotes self-renewal of LGR5 stem cells

a Schematic of the targeting strategy to interfere MBD3 expression. **b** Western blot showing knockdown of MBD3 protein in clone #14. Results reproducible for at least two biological replicates. **c** RT-qPCR quantification of MBD3 and LGR5 expression. Two-way ANOVA with Dunnett's multiple comparisons test; data are presented as mean ± SD; representative experiment showing *n* = 3 samples from each condition. **d** Representative confocal images of LGR5-mNeonGreen stem cells and Paneth cells (DEFA5) in organoids cultured in conditions as indicated. Representative images from three independent experiments. Scale bar, 50μm. **e** Relative fluorescence intensity in organoid of (**d**). One-way ANOVA with Dunnett's multiple comparisons test; data are presented as mean ± SD; representative experiment showing *n* = 4 samples from each condition. Source data for this Figure are provided as a Source Data file.

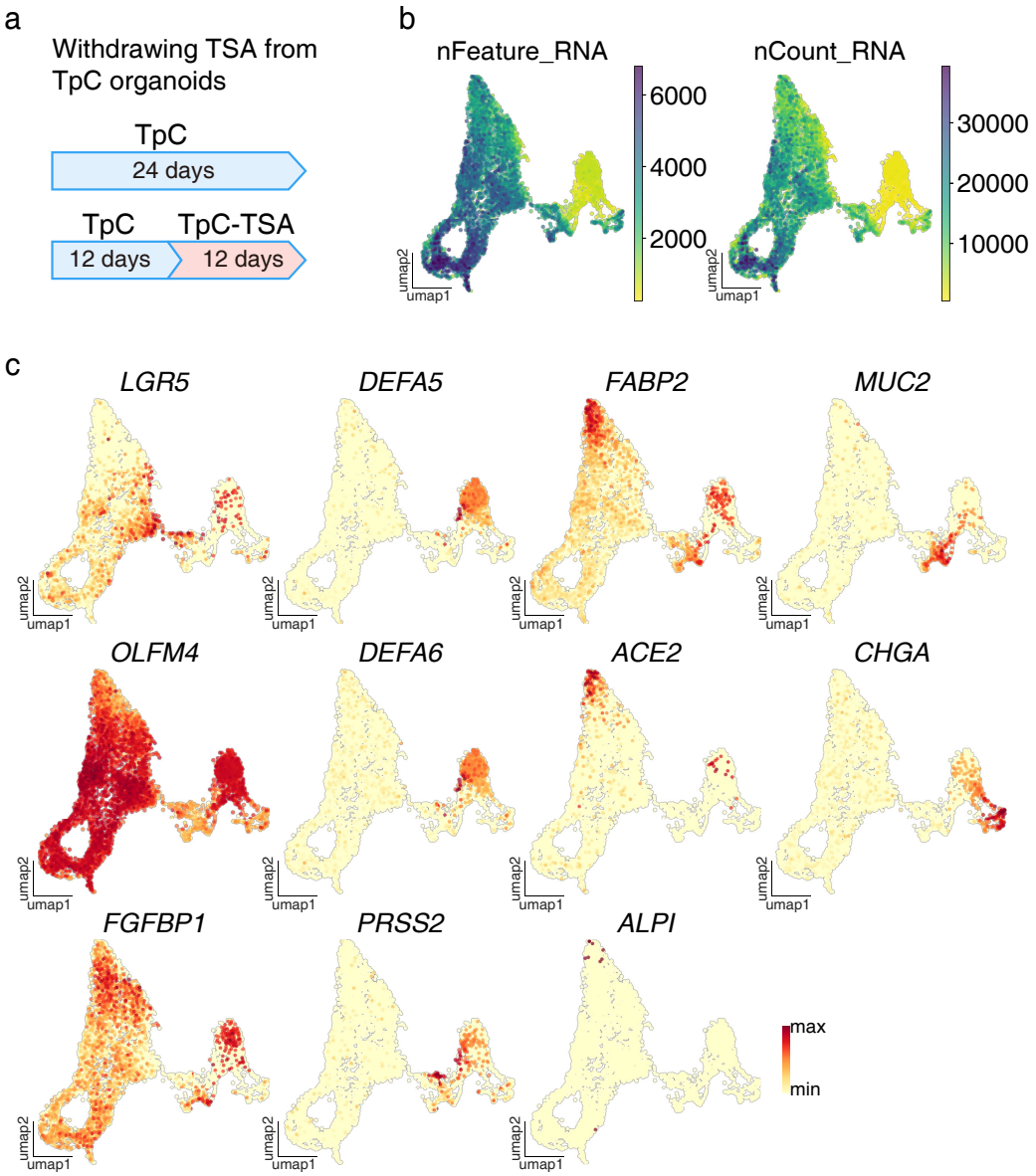

Supplementary Fig. 14 | Effects of TSA withdrawal on TpC organoids.

a Schematic representation of the experimental design, showing the withdrawal of TSA from TpC organoids. Organoids were cultured in TpC conditions for 24 days or in TpC conditions for 12 days followed by TpC-TSA conditions for another 12 days. **b** UMAP plots showing the distribution of nFeature_RNA and nCount_RNA in the organoids. The color gradient represents the number of features (left) and the RNA count (right). **c** UMAP plots displaying the expression patterns of cell type specific marker genes in the organoids after TSA withdrawal. The genes include *LGR5* and *OLFM4* (stem cell marker), *DEFA5*, *DEFA6* and *PRSS2* (Paneth cell markers), *FABP2*, *ACE2* and *ALPI* (enterocyte markers), *MUC2* (goblet cell marker), *CHGA* (enteroendocrine cell marker) The color gradient represents expression levels, from minimum (yellow) to maximum (red).

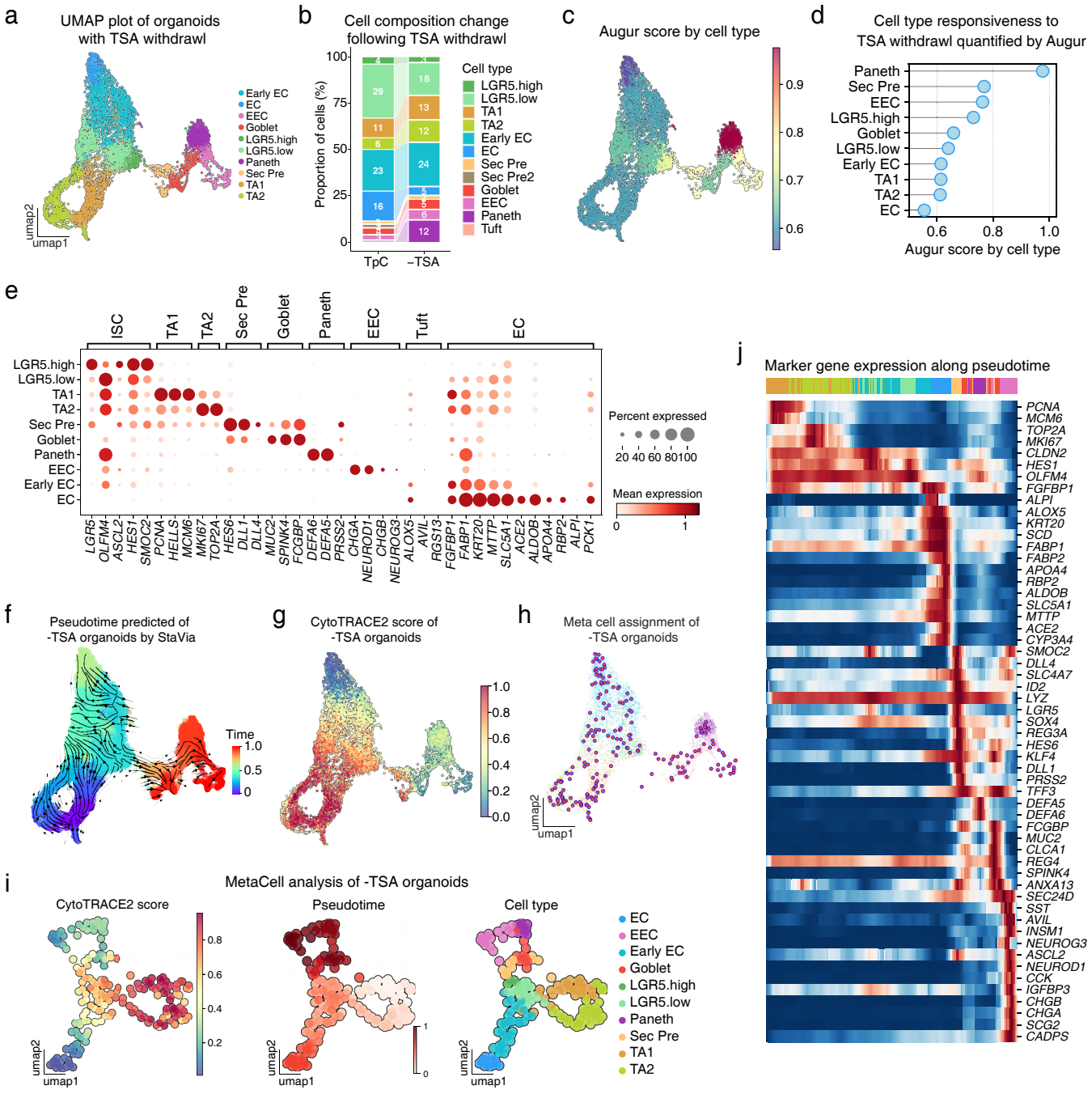
a
UMAP plot of organoids with TSA withdrawl
Early EC
EC
EEC
Goblet
LGR5.high
LGR5.low
Paneth
Sec Pre
TA1
TA2
umap2
umap1
b
Cell composition change following TSA withdrawl
Proportion of cells (%)
100
75
50
25
0
TpC
−TSA
Cell type
LGR5.high
LGR5.low
TA1
TA2
Early EC
EC
Sec Pre
Sec Pre2
Goblet
EEC
Paneth
Tuft
c
Augur score by cell type
0.9
0.8
0.7
0.6
d
Cell type responsiveness to TSA withdrawl quantified by Augur
Paneth
Sec Pre
EEC
LGR5.high
Goblet
LGR5.low
Early EC
TA1
TA2
EC
0.6
0.8
1.0
Augur score by cell type
e
ISC
TA1
TA2
Sec Pre
Goblet
Paneth
EEC
Tuft
EC
LGR5.high
LGR5.low
TA1
TA2
Sec Pre
Goblet
Paneth
EEC
Early EC
EC
LGR5
OLFM4
ASCL2
HES1
SMOC2
PCNA
HELLS
MCM6
MKI67
TOP2A
HES6
DLL1
DLL4
MUC2
SPINK4
FCGBP
DEFA6
DEFA5
PRSS2
CHGA
NEUROD1
CHGB
NEUROG3
ALOX5
AVIL
RGS13
FGFBP1
FABP1
KRT20
MTTP
SLC5A1
ACE2
ALDOB
APOA4
RBP2
ALPI
PCK1
Percent expressed
20 40 60 80100
Mean expression
0
1
f
Pseudotime predicted of -TSA organoids by StaVia
Time
1.0
0.5
0
g
CytoTRACE2 score of -TSA organoids
1.0
0.8
0.6
0.4
0.2
0.0
h
Meta cell assignment of -TSA organoids
umap2
umap1
i
MetaCell analysis of -TSA organoids
CytoTRACE2 score
0.8
0.6
0.4
0.2
umap2
umap1
Pseudotime
1
0
umap2
umap1
Cell type
umap2
umap1
EC
EEC
Early EC
Goblet
LGR5.high
LGR5.low
Paneth
Sec Pre
TA1
TA2
j
Marker gene expression along pseudotime
PCNA
MCM6
TOP2A
MKI67
CLDN2
HES1
OLFM4
FGFBP1
ALPI
ALOX5
KRT20
SCD
FABP1
FABP2
APOA4
RBP2
ALDOB
SLC5A1
MTTP
ACE2
CYP3A4
SMOC2
DLL4
SLC4A7
ID2
LYZ
LGR5
SOX4
REG3A
HES6
KLF4
DLL1
PRSS2
TFF3
DEFA5
DEFA6
FCGBP
MUC2
CLCA1
REG4
SPINK4
ANXA13
SEC24D
SST
AVIL
INSM1
NEUROG3
ASCL2
NEUROD1
CCK
IGFBP3
CHGB
CHGA
SCG2
CADPS

Supplementary Fig. 15 | Cellular and molecular changes in organoids following TSA withdrawal.

a UMAP plot of -TSA organoids showing distinct cell clusters based on cell type. **b** Bar plot showing the change in cell composition following TSA withdrawal. Proportions of each cell type in TpC and -TSA conditions are indicated. **c** UMAP plot displaying Augur scores by cell type, indicating the cell types' responsiveness to TSA withdrawal. **d** Quantifying cell type responsiveness to TSA removal using Augur scores as in (c). **e** Expression of marker genes across different cell types in -TSA organoids. **f** Pseudotime trajectory of -TSA organoids predicted by StaVia. **g** UMAP plot displaying CytoTRACE2 scores of -TSA organoids. **h** Meta cell assignment of -TSA organoids using SEACells, showing the clustering of cells into distinct meta cells based on transcriptomic similarity. **i** UMAP plots of -TSA organoids showing (from left to right) CytoTRACE2 scores, pseudotime score, and cell type clustering. **j** Heatmap of marker gene expression along pseudotime in -TSA organoids, with genes and cell types indicated. Color bar indicates cell types as in (**i**). The color gradient represents expression levels from low (blue) to high (red).

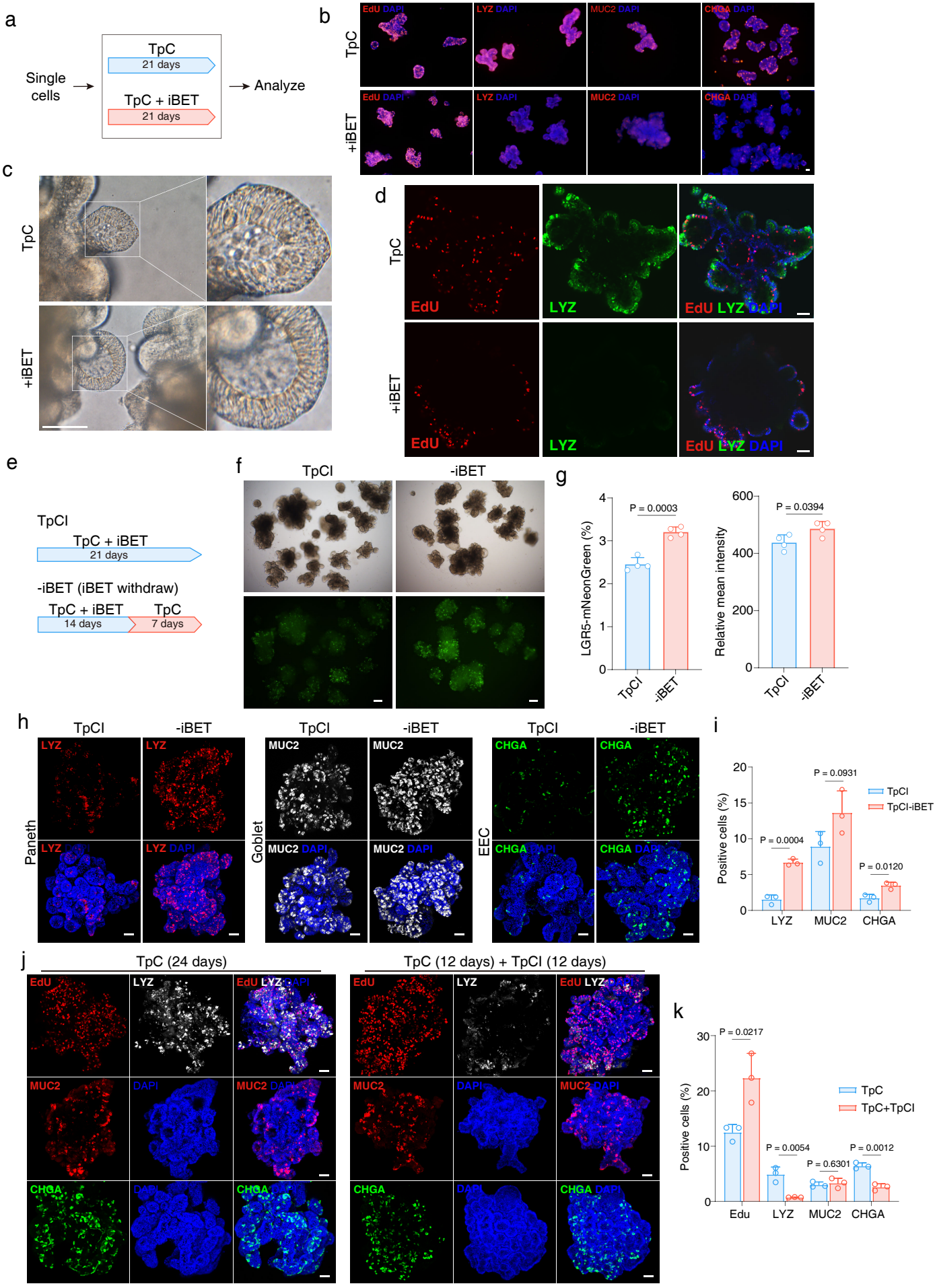
a
Single cells
TpC
21 days
TpC + iBET
21 days
Analyze
b
TpC
+iBET
EdU DAPI
LYZ DAPI
MUC2 DAPI
CHGA DAPI
c
TpC
+iBET
d
TpC
+iBET
EdU
LYZ
EdU LYZ DAPI
e
TpCI
TpC + iBET
21 days
-iBET (iBET withdraw)
TpC + iBET
14 days
TpC
7 days
f
TpCI
-iBET
g
LGR5-mNeonGreen (%)
P = 0.0003
Relative mean intensity
P = 0.0394
TpCI
-iBET
h
TpCI
-iBET
Paneth
Goblet
EEC
LYZ
MUC2
CHGA
i
Positive cells (%)
P = 0.0004
P = 0.0931
P = 0.0120
TpCI
TpCI-iBET
LYZ
MUC2
CHGA
j
TpC (24 days)
TpC (12 days) + TpCI (12 days)
EdU
LYZ
MUC2
CHGA
DAPI
k
Positive cells (%)
P = 0.0217
P = 0.0054
P = 0.6301
P = 0.0012
TpC
TpC+TpCI
Edu
LYZ
MUC2
CHGA

Supplementary Fig. 16 | iBET-151 promotes proliferation and inhibits differentiation on single cells or established organoids.

a Schematic of organoid culture conditions for experiments in (**b**-**d**). **b** EdU and immunofluorescence staining of Paneth cells (LYZ), goblet cells (MUC2), and enteroendocrine cells (CHGA) of organoids cultured in conditions as indicated. **c** Representative images of budding crypts of organoids cultured in conditions as indicated. **d** Co-localization of Paneth cell marker LYZ and EdU in organoids. Representative images of (**a**-**c**) were from three independent experiments. **e** Schematic of organoid culture conditions for experiments in (**f**-**i**). **f** Representative brightfield and LGR5-mNeonGreen fluorescence images of organoids cultured in conditions as indicated. Representative images from four independent experiments. **g** Quantification of LGR5-mNeonGreen cell percentage and relative mean fluorescent intensity of organoids cultured in conditions as indicated. Two-tailed unpaired t-test; data are presented as mean ± SD; representative experiment showing n = 4 samples from each condition. **h** EdU and immunofluorescence staining of Paneth cells (LYZ), goblet cells (MUC2), and enteroendocrine cells (CHGA) in organoid cultures as in (**e**). EdU was administered for 1 hour before staining. **i** Quantification of LYZ, MUC, and CHGA positive cells as shown in (**h**). Two-tailed unpaired t-test; data are presented as mean ± SD; n = 3 samples. **j** EdU and immunofluorescence staining of Paneth cell (LYZ), goblet cell (MUC2), and enteroendocrine (CHGA) staining in organoid cultures as indicated. Representative images of (**h** and **j**) were from three independent experiments. **k** Quantification of EdU, LYZ, MUC2, and CHGA positive cells in organoids as in (**j**). Two-tailed unpaired t-test; data are presented as mean ± SD; n = 3 samples. Scale bars, (**b**, **c** and **f**), 200 μm; (**d**, **h** and **j**), 50 μm. Source data for this Figure are provided as a Source Data file.

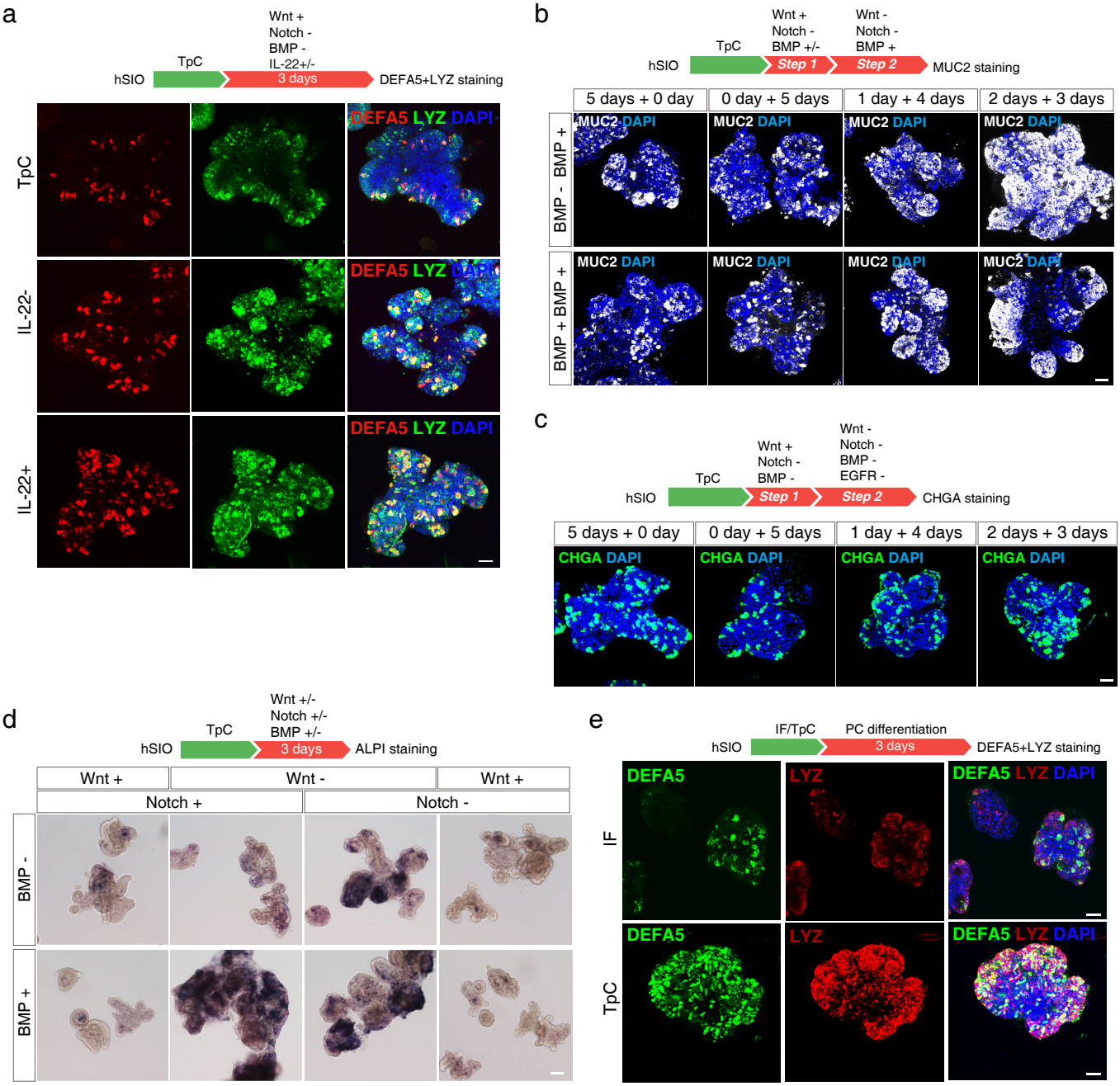

Supplementary Fig. 17 | Cell fate regulation by combinations of niche signals.

a Representative confocal images showing Paneth cell differentiation (marked by LYZ and DEFA5) in organoids with IL-22 modulation. **b** Representative confocal images showing goblet cell differentiation (marked by MUC2) in organoids with BMP pathway modulation and a stepwise differentiation protocol. **c** Representative confocal images showing enteroendocrine cell differentiation (CHGA) in organoids with a stepwise differentiation protocol. (**a**-**c**), Scale bars, 50 μm. **d** ALPI staining showing enterocyte differentiation in organoids with modulation of Wnt, Notch, and BMP signaling as indicated. Scale bars, 200 μm. **e** Representative confocal images showing Paneth cell (DEFA5 and LYZ) in organoids cultured in IF and TpC condition and following induced Paneth cell differentiation for 3 days. All the representative images of this Figure were from three independent experiments. Scale bars, 50 μm.

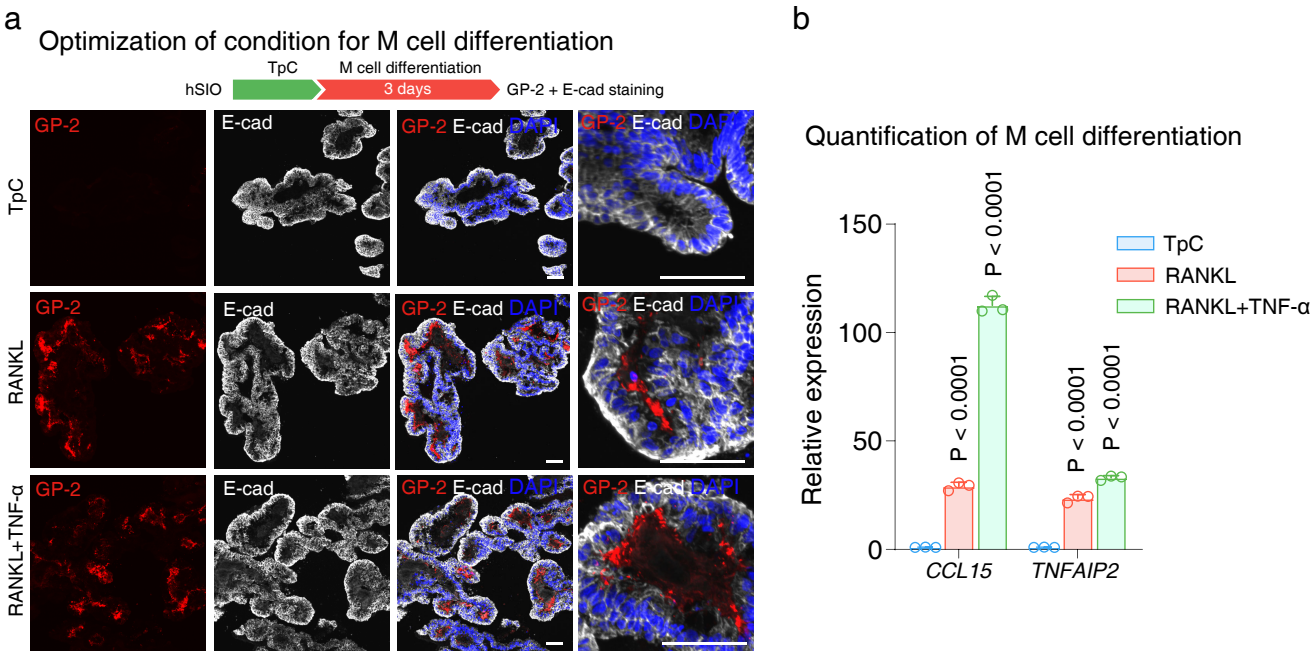

Supplementary Fig. 18 | Directed differentiation of M cells from TpC organoids.

a Representative confocal images showing M cells differentiation (GP-2) and E-cadherin (E-cad) in organoids with conditions previously published in mouse organoid. Representative images from three independent experiments. Scale bars, 50 μm. **b** RT-qPCR quantification of M cell markers *CCL15* and *TNFAIP2* in organoids as in (**a**). Two-way ANOVA with Dunnett's multiple comparisons test; data are presented as mean ± SD; representative experiment showing *n* = 3 samples from each condition. Source data are provided as a Source Data file.

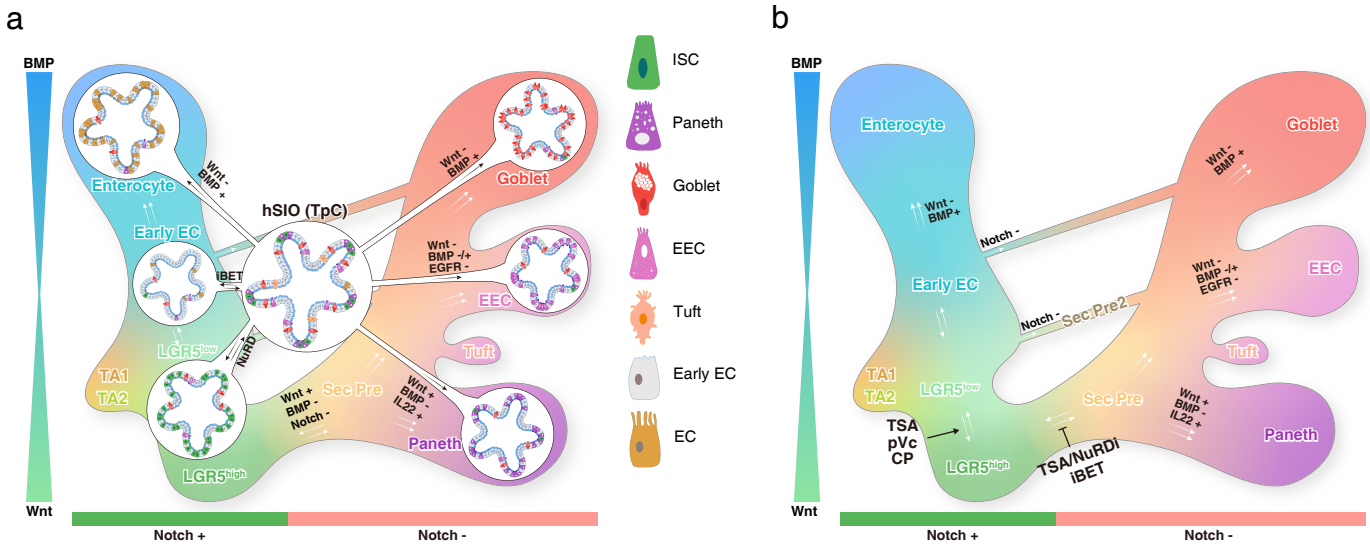

Supplementary Fig. 19 | Model depicting establishing and modulating cell fate equilibrium in human intestinal organoids.

a The combination of factors in the TpC condition maintains human intestinal organoids in a balanced state between self-renewal and differentiation. The addition of iBET shifts this balance towards enterocyte lineage. The balance can be further shifted towards enhanced differentiation of each intestinal epithelial cell type through modulating the combination of niche signaling, including IL-22, Wnt, Notch, BMP, EGFR pathways, in a stepwise manner. **b** Proposed function of small molecules TSA, pVc, CP, and iBET.

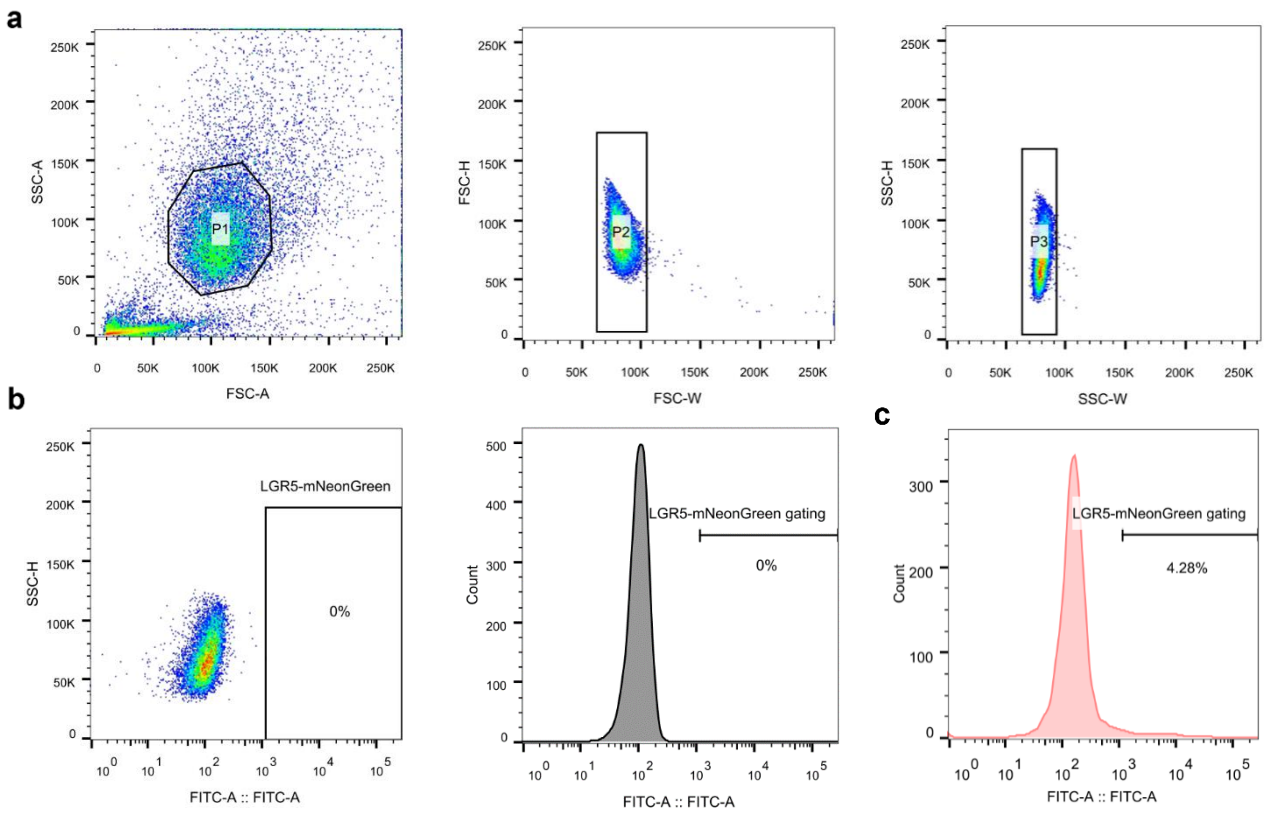

Supplementary Fig. 20 | Flow cytometry gating strategy.

a Cell selection and debris removal: Dissociated hSIO cells were first identified based on forward scatter (FSC) vs. side scatter (SSC) to remove debris (left panel). Subsequently, doublets were excluded by evaluating FSC-height (FSC-H) vs. FSC-width (FSC-W) (medium panel) and SSC-height (FSC-H) vs. SSC-width (SSC-W) (right panel). **b** Gating LGR5-mNeonGreen population in Non-reporter hSIO cells: in hSIO cells without mNeonGreen reporter expression, LGR5-mNeonGreen population were gated based on their FITC fluorescence intensity. **c** Gating LGR5 population in mNeonGreen reporter hSIO as an example: for LGR5-mNeonGreen hSIO cells, the LGR5-mNeonGreen gate established in step (**b**) were applied. The LGR5 population was further selected by assessing FITC fluorescence from the mNeonGreen reporter.

Supplementary Table 1 | CRISPR target sites, homology arms, knock-in sequence and PCR primers used in the study.

Target Gene	gRNA location (human hg38)	gRNA Sequences (5' to 3')
LGR5-1	chr12: 71,584,804-71,584,823	1#: GTAATTAATAAGAAGAGCTG
LGR5-2	chr12: 71,584,726-71,584,745	2#: TGTCTCTAATTAATATGTGA
MBD3-4	chr19: 1,584,627-1,584,646	4#: GATGGACGCCGTCTGGCGCA

Homology arms	Genomic location (human hg38)	Span (bp)
LGR5-5'arm	chr12: 71,583,717-71,584,731	1015
LGR5-3'arm	chr12: 71,584,732-71,585,979	1248

LGR5-mNeonGreen KI	Sequence (5'-3') (**P2A+**mNeonGreen**)**
	GCAACAAACTTCTCTCTGCTGAAACAAGCCGGAGATGTCGAAG
	AGAATCCTGGACCGATGGTGAGCAAGGGCGAGGAGGATAACAT
	GGCCTCTCTCCCAGCGACACATGAGTTACACATCTTTGGCTCCAT
	CAACGGTGTGGACTTTGACATGGTGGGTCAGGGCACCGGCAAT
	CCAAATGATGGTTATGAGGAGTTAAACCTGAAGTCCACCAAGGGT
	GACCTCCAGTTCTCCCCCTGGATTCTGGTCCCTCATATCGGGTAT
	GGCTTCCATCAGTACCTGCCCTACCCTGACGGGATGTCGCCTTT
	CCAGGCCGCCATGGTAGATGGCTCCGGCTACCAAGTCCATCGCA
	CAATGCAGTTTGAAGATGGTGCCTCCCTTACTGTTAACTACCGCT
	ACACCTACGAGGGAAGCCACATCAAAGGAGAGGCCCAGGTGAA
	GGGGACTGGTTTCCCTGCTGACGGTCCTGTGATGACCAACTCGC
	TGACCGCTGCGGACTGGTGCAGGTCGAAGAAGACTTACCCCAA
	CGACAAAACCATCATCAGTACCTTTAAGTGGAGTTACACCACTGG
	AAATGGCAAGCGCTACCGGAGCACTGCGCGGACCACCTACACC
	TTTGCCAAGCCAATGGCGGCTAACTATCTGAAGAACCAGCCGAT
	GTACGTGTTCCGTAAGACGGAGCTCAAGCACTCCAAGACCGAGC
	TCAACTTCAAGGAGTGGCAAAAGGCCTTTACCGATGTGATGGGC
	ATGGACGAGCTGTACAAGTAA

LGR5-KI	PCR primers	Sequences (5' to 3')
	F1	TGGCATCCTAAATAAAGAGACAAAAGGGTA
	R1	GTGCGATGGACTTGGTAGCC
	F2	TCCCTGCTGACGGTCCTGT
	R2	CTTAAATAGCAGGCCGGGCG
	F3	AGCCTGAGAAAGCAAACC
	R3	TCTGAGGAAAGGCAAAGG

Supplementary Table 2 | Proteins and small molecules used in this study.

Name	Source	Identifier
Recombinant Murine EGF	Peprotech	Cat#315-09
Recombinant Human IGF-I	Peprotech	Cat#100-11
Recombinant Human FGF-basic	Peprotech	Cat#100-18C
DMH1	ApexBio	Cat#B3686
Gastrin I	MCE	Cat#HY-P1097
A83-01	ApexBio	Cat#A3133
CHIR-99021 (CHIR)	ApexBio	Cat#A3011
Trichostatin A (TSA)	ApexBio	Cat#A8183
2-phospho-L-ascorbic acid trisodium salt (pVc)	Sigma	Cat#49752
CP673451 (CP)	TargetMol	Cat#T6091
Y-27632 dihydrochloride	TargetMol	Cat#T1725
Valproic acid sodium salt (VPA)	Sigma	Cat#P4543
Tubastatin A HCl	ApexBio	Cat#A8547
LMK235	TargetMol	Cat#T6061
CAY10683	Selleck	Cat#S7595
Gefitinib	TargetMol	Cat#T1181
DAPT	TargetMol	Cat#T6202
IWR-1	TargetMol	Cat#T2651
SJ000291942	TargetMol	Cat#T4662
iBET151	Selleck	Cat#S2780
KCC-07	TargetMol	Cat#T8554
Recombinant human IL-22	PrimeGene	Cat#101-22
Recombinant human RANKL	Peprotech	Cat#310-01
Recombinant human TNF-α	Peprotech	Cat#300-01A

Supplementary Table 3 | Antibodies used in this study.

Antibody	Vendor	Identifier
Rabbit anti-Lysozyme	Invitrogen	Cat#PA5-16668, RRID:AB_10984852
Mouse anti-Chr-A (C-12)	Santa Cruz	Cat#sc-393941, RRID:AB_2801371
Mouse anti-Mucin 2 (Ccp58)	Santa Cruz	Cat#sc-7314, RRID:AB_627970
Mouse anti-α-defensin 5 (8c8)	Santa Cruz	Cat#sc-53997, RRID:AB_2091709
Rabbit anti-OLFM4(D1E4M)	CST	Cat#14369, RRID:AB_2798465
Rat anti-Somatostatin, Clone YC7	Millipore	Cat#MAB354, RRID:AB_2255365
Mouse anti-Glucagon (C-11)	Santa Cruz	Cat#sc-514592, RRID:AB_2629431
Mouse anti-GP2	MBL	Cat#D277-3, RRID:AB_10598500
Rabbit anti-E-cadherin	Proteintech	Cat#20874-1-AP, RRID:AB_10697811
Mouse anti-MBD2/3 (D-7)	Santa Cruz	Cat#sc-271562, RRID:AB_10659107
Rabbit anti-GAPDH (D16H11)	CST	Cat#5174T, RRID:AB_10622025
Mouse anti-ALPI	Santa Cruz	Cat#sc-271431, RRID:AB_10649489
Donkey anti-Mouse IgG (H+L), Alexa Fluor™ Plus 488	Invitrogen	Cat#A32766, RRID:AB_2762823
Donkey anti-Rabbit IgG (H+L), Alexa Fluor™ Plus 488	Invitrogen	Cat#A32790, RRID:AB_2762833
Donkey anti-Mouse IgG (H+L), Alexa Fluor™ Plus 555	Invitrogen	Cat#A32773, RRID:AB_2762848
Donkey anti-Rabbit IgG (H+L), Alexa Fluor™ Plus 555	Invitrogen	Cat#A32794, RRID:AB_2762834
Goat anti-Rat IgG (H+L), Alexa Fluor™ 555	Invitrogen	Cat#A-21434, RRID:AB_2535855
Donkey anti-Rabbit IgG (H+L), Alexa Fluor™ Plus 647	Invitrogen	Cat#A32795, RRID:AB_2762835
Donkey anti-Mouse IgG (H+L), Alexa Fluor™ 647	Invitrogen	Cat#A-31571, RRID:AB_162542

Supplementary Table 4 | Primers used for quantitative RT-PCR.

Genes	Primer Sequences (5' to 3')
GAPDH	F-GGAGCGAGATCCCTCCAAAAT
	R-GGCTGTTGTCATACTTCTCATGG
LGR5	F-CTCCCAGGTCTGGTGTGTTG
	R-GAGGTCTAGGTAGGAGGTGAAG
OLFM4	F-ACTGTCCGAATTGACATCATGG
	R-TTCTGAGCTTCCACCAAAACTC
BMI1	F-CGTGTATTGTTCGTTACCTGGA
	R-TTCAGTAGTGGTCTGGTCTTGT
LYZ	F-CTTGTCCTCCTTTCTGTTACGG
	R-CCCCTGTAGCCATCCATTCC
DEFA5	F-AGACAACCAGGACCTTGCTAT
	R-GGAGAGGGACTCACGGGTAG
DEFA6	F-CTGAGCCACTCCAAGCTGAG
	R-GTTGAGCCCAAAGCTCTAAGAC
REG3G	F-GGTGAGGAGCATTAGTAACAGC
	R-CCAGGGTTTAAGATGGTGGAGG
MUC2	F-GAGGGCAGAACCCGAAACC
	R-GGCGAAGTTGTAGTCGCAGAG
CLCA1	F-ACAACAATGGCTATGAAGGCA
	R-GGTCTCAAGTTTTGGTCTCACAT
CHGA	F-TAAAGGGGATACCGAGGTGATG
	R-TCGGAGTGTCTCAAAACATTCC
SST	F-ACCCAACCAGACGGAGAATGA
	R-GCCGGGTTTGAGTTAGCAGA
GCG	F-CTGAAGGGACCTTTACCAGTGA
	R-CCTGGCGGCAAGATTATCAAG
NEUROG3	F-CTAAGAGCGAGTTGGCACTGA
	R-GAGGTTGTGCATTCGATTGCG
ALPI	F-TGAGGGTGTGGCTTACCAG
	R-GATGGACGTGTAGGCTTTGCT
SMOC2	F-TTCTCGGCGCTCACGTTTTT
	R-GTTGAAATTCACAACGGGAAAGG
TFF3	F-CCAAGCAAACAATCCAGAGCA
	R-GCTCAGGACTCGCTTCATGG
TPH1	F-ACGTCGAAAGTATTTTGCGGA
	R-ACGGTTCCCCAGGTCTTAATC

ACE2	F-CGAAGCCGAAGACCTGTTCTA
	R-GGGCAAGTGTGGACTGTTCC
FABP1	F-ATGAGTTTCTCCGGCAAGTACC
	R-CTCTTCCGGCAGACCGATTG
CCL15	F-TCCCAGGCCCAGTTCATAAAT
	R-TGCTTTGTGAGATGTAGGAGGT
TNFAIP2	F-GGCCAATGTGAGGGAGTTGAT
	R-CCCGCTTTATCTGTGAGCCC
MBD3	F-CTGAGCACCTTCGACTTCCG
	R-CCGGCTGCTTGAAGATGGA